


Asgard archaea modulate potential methanogenesis substrates in wetland soil

Working Paper**Author(s):**

Valentin-Alvarado, Luis E.; Appler, Kathryn E.; Appler, Kathryn E.; [Schoelmerich, Marie](#) ; West-Roberts, Jacob; Kivenson, Veronika; Crits-Christoph, Alexander; Ly, Lynn; Sachdeva, Rohan; Savage, David F.; Baker, Brett J.; Banfield, Jillian F.

Publication date:

2023-11

Permanent link:

<https://doi.org/10.3929/ethz-b-000668192>

Rights / license:

[Creative Commons Attribution-NonCommercial-NoDerivatives 4.0 International](#)

Originally published in:

bioRxiv, <https://doi.org/10.1101/2023.11.21.568159>

1 Asgard archaea modulate potential methanogenesis substrates in wetland soil

2
3 Luis E. Valentin-Alvarado^{1,2,†}, Kathryn E. Appler^{3,†}, Valerie De Anda^{3,4}, Marie C.
4 Schoelmerich^{1,‡}, Jacob West-Roberts⁵, Veronika Kivenson⁹, Alexander Crits-Christoph^{1,2,§}, Lynn
5 Ly⁶, Rohan Sachdeva¹, David F. Savage^{1,7}, Brett J. Baker^{3,4}, and Jillian F. Banfield^{1,4,8,9,*}

7 Affiliations:

8 ¹ Innovative Genomics Institute, University of California; Berkeley, 94720, California, USA

9 ² Department of Plant and Microbial Biology, University of California; Berkeley, CA, USA

10 ³ Department of Marine Science, University of Texas at Austin; Marine Science Institute, Port
11 Aransas, TX, USA

12 ⁴ Department of Integrative Biology, University of Texas at Austin; Austin, TX, USA

13 ⁵ Environmental Science, Policy and Management, University of California; Berkeley, CA, USA

14 ⁶ Oxford Nanopore Technologies Inc; New York, NY, USA

15 ⁷ Howard Hughes Medical Institute, University of California; Berkeley, California, USA

16 ⁸ Department of Microbiology, Biomedicine Discovery Institute; Monash University, VIC, AUS

17 ⁹ Earth and Planetary Science, University of California; Berkeley, CA, USA

18
19 †These authors contributed equally to this work

20 ‡Current affiliation: Department of Environmental Systems Sciences; ETH Zürich, Switzerland

21 §Current affiliation: Cultivarium; Watertown, MA, USA

22
23 * Corresponding author: jbanfield@berkeley.edu

25 Abstract:

26 The roles of Asgard archaea in eukaryogenesis and marine biogeochemical cycles are well studied,
27 yet their contributions in soil ecosystems are unknown. Of particular interest are Asgard archaeal
28 contributions to methane cycling in wetland soils. To investigate this, we reconstructed two
29 complete genomes for soil-associated Atabayarchaeia, a new Asgard lineage, and the first
30 complete genome of Freyarchaeia, and defined their metabolism *in situ*. Metatranscriptomics
31 highlights high expression of [NiFe]-hydrogenases, pyruvate oxidation and carbon fixation via the
32 Wood-Ljungdahl pathway genes. Also highly expressed are genes encoding enzymes for amino
33 acid metabolism, anaerobic aldehyde oxidation, hydrogen peroxide detoxification and glycerol and
34 carbohydrate breakdown to acetate and formate. Overall, soil-associated Asgard archaea are
35 predicted to be non-methanogenic acetogens, likely impacting reservoirs of substrates for methane
36 production in terrestrial ecosystems.

38 One-Sentence Summary:

39 Complete genomes of Asgard archaea, coupled with metatranscriptomic data, indicate roles in
40 production and consumption of carbon compounds that are known to serve as substrates for
41 methane production in wetlands.

42
43
44
45
46
47
48
49
50
51
52
53
54
55
56
57
58
59
60
61
62
63
64
65
66
67
68
69
70
71
72
73
74
75
76
77
78
79
80
81
82
83
84
85
86
87

Introduction

Wetland soils are hotspots for methane production by methanogenic archaea. The extent of methane production depends in part on the availability of substrates for methanogenesis (e.g., formate, formaldehyde, methanol, acetate, hydrogen), compounds that are both produced and consumed by co-existing microbial community members. Among the groups of organisms that coexist with methanogens are Asgard archaea, of recent interest from the perspective of eukaryogenesis (1–4). To date, numerous lineages of Asgard archaea have been reported from anaerobic, sedimentary freshwater, marine, and hydrothermal environments (1–15). Predictions primarily from draft metagenome-assembled genomes (MAGs) indicate metabolic diversity and flexibility that may enable them to occupy these diverse ecological niches. It appears that Asgard archaea are not capable of methane production since they lack the key canonical methyl-coenzyme M reductase (MCR). Although a few complete genomes for Asgard from hydrothermal and geothermal environments have been reported (9, 15–17), most metabolic analyses of Asgard archaea are limited by reliance on partial genomes. To date, no Asgard genomes from non-estuarine wetland soils have been reported. Thus, nothing is known about the ways in which Asgard archaea directly (via methane production) or indirectly (via metabolic interactions) impact methane cycling in wetlands.

To investigate the roles of Asgard archaea in carbon cycling in wetland soil, we reconstructed two complete genomes for a newly defined group, here named Atabeyarchaeia, and one complete genome for a group named Freyarchaeia. Freyarchaeia MAGs were originally reconstructed from Guaymas Basin, located in the Gulf of California, México (14), and from Jinze Hot Spring (Yunnan, China) (4). Subsequently, another group used the original data to recover similar genomes and referred to them as Jordarchaeia (18). Here, we retain the original nomenclature. The genomes for soil Asgard archaea were initially reconstructed by manual curation of Illumina short read assemblies and then validated using both Nanopore and PacBio long reads. These fully curated genomes enabled us to perform comprehensive metabolic analyses, without the risks associated with reliance on draft genomes, and provided context for metatranscriptomic measurements of their *in situ* activity. Our integrated analysis of gene expression and metabolic predictions revealed roles for Atabeyarchaeia and Freyarchaeia in the production and consumption of carbon compounds that can serve as substrates for methanogenesis by coexisting methanogenic archaea.

88 Results

89

90 *Complete genomes and phylogenetic placement of Asgard archaea from wetland soil*

91

92 We analyzed Illumina metagenomic data from samples collected from 20 cm to 175 cm depth in
93 the soil of a wetland located in Lake County, California, USA. We previously reported
94 megaphages (19) and *Methanoperedens* archaea and their 1 Mb-scale “Borg” extrachromosomal
95 elements from this site (20). From the metagenomic analyses conducted at this site, we determined
96 that archaea account for >45% of the total community below a depth of 60 cm. Archaeal groups
97 detected include members of the Asgardarchaeota, Bathyarchaeia, Methanosarcinia,
98 Nitrososphaeria, Thermoplasmata, Micrarchaeia, Diapherotrites, Aenigmataarchaeia,
99 Methanomicrobia, Aenigmarchaeia, Nanoarchaeia, Hadarchaeia and Methanomethylia (**Fig. 1A-**
100 **B**)

101 From 60 cm, 80 cm, and 100 cm deep wetland soil, we recovered four draft Asgard
102 genomes, three of which were manually curated to completion using methods described previously
103 (21). Taxonomic classification using the Silva DB placed the 3,576,204 bp genome as Freyarchaeia.
104 16S rRNA gene sequence analysis showed the two other complete genomes were distinct from
105 Freyarchaeia (16S rRNA genes are <75% identical), thus representing organisms from a separate,
106 new lineage. These genomes are 2,808,651 and 2,756,679 bp in length (**table S1**) with an average
107 amino acid identity (AAI) of ~70% (**table S2**).

108 Phylogenetic analyses using several sets of marker genes (“see materials and methods”)
109 placed our two novel complete genomes in a monophyletic group within the Asgard clade as a
110 sister group to Freyarchaeia (**Fig. 1C**). We performed phylogenetic analyses using concatenated
111 marker sets of 47 arCOG and 15 ribosomal protein (RP15) gene cluster (**fig. S1**), as well as 16S
112 rRNA (**fig. S2**). The new genomes share only 40-45% AAI when compared to other Asgard
113 genomes, consistent with their assignment to a new phylum. Although our analyses provide
114 evidence for distinction at the phylum level, we chose to adhere to the Genome Taxonomy
115 Database (GTDB) for standardized microbial genome nomenclature (**table S3**). Here, we propose
116 the name *Candidatus* “Atabeyarchaeia” for this new group, where ‘Atabey’ is a goddess in of Taíno
117 Puerto Rican mythology. Atabeyarchaeia is represented by the complete Atabeyarchaeia group 1
118 (Atabeya-1) and group 2 (Atabeya-2) genomes. Included in this group are 2 MAGs from a highly
119 fragmented, partial Asgard Lake Cootharaba Group (ALCG) draft genome (12). The cumulative
120 GC skew of the Freyarchaeia and Atabeyarchaeia genomes is consistent with bidirectional
121 replication. This style of replication is typical of bacterial genomes but has not been widely
122 reported in Archaea, and has never been described in the Asgard group (**Fig. 1D and fig. S3**).

123 Unexpectedly, we found that 92% to 95% of tRNA genes from all three genomes contain
124 at least one intron. This contrasts with the general estimate that 15% of archaeal tRNA harbor
125 introns (22), and with Thermoproteales (another order of archaea), where 70% of the tRNAs
126 contain introns (23). In total, there are 228 tRNA introns across the three new Asgard genomes
127 (**table S4**). Unlike most archaeal tRNA introns that occur in the anticodon loop at position 37 / 38
128 (24, 25), Atabeyarchaeia and Freyarchaeia introns often occur at non-canonical positions, and over
129 half of their tRNA genes have multiple introns (**table S4**).

130 Subsequently, we acquired and independently assembled Oxford Nanopore and PacBio
131 long-reads from a subset of the samples to generate three circularized genomes that validate the
132 overall topology of all three curated Illumina read-based genomes (**fig. S4, table S1**). These
133 complete genomes allowed us to genomically describe two Atabeya-2 strain variants from 100 cm

134 and 175 cm depth soil. In addition, we used Illumina reads to curate a draft Nanopore genome for
135 another Atabayarchaeia species, Atabeya-3, from 75 cm and 175 cm depth soil (**fig. S5**). The
136 Atabayarchaeia-3 genome is most closely related to the Asgard Lake Cootharaba Group (ALCG)
137 fragments (18). To further solidify the phylogenetic position of Atabayarchaeia, we included the
138 Atabayarchaeia-3 genome and another draft genome (Atabayarchaeia-4) from Illumina reads in
139 the phylogenetic analysis.

140 Using the Asgard clusters of orthologous genes (AsCOGS) database and functional
141 classification, we identified eukaryotic signature proteins (ESPs) in the complete and public
142 genomes of Atabayarchaeia and Freyarchaeia (2, 3). Atabayarchaeia and Freyarchaeia genomes
143 had the highest percentage of hits for 'Intracellular trafficking, secretion, and vesicular transport'
144 (U) among the AsCOG functional classes, accounting for 84.3% of the hits to the database. Within
145 this class, we identified key protein domains such as Adaptin, ESCRT-I-III complexes, Gelsolin
146 family protein, Longin domain, Rab-like GTPase, Ras family GTPase, and Roadblock/LC7
147 domain (**table S5, fig. S6**). The 'Post Translational modification, protein turnover, and chaperones'
148 category (O) followed with a count of 101 (15.8%), highlighting domains like Ubiquitin,
149 Jab1/MPN domain-containing protein, and the RING finger domain. The presence of ESPs in the
150 newly described Atabayarchaeia lineage and their presence in Freyarchaeia aligns with previous
151 findings for Asgardarchaeota (1, 3, 4).

152

153 *Expression of energy conservation pathways constrain key metabolisms in situ*

154

155 We analyzed the metabolic potential of the three complete genomes and investigated their activity
156 *in situ* through metatranscriptomics of soil samples (“**see materials and methods**”, **Fig. 2, table**
157 **S6, table S7**). The metatranscriptomic data indicate high expression of genes involved in key
158 energy conservation pathways (**Fig. 3A**). Most highly transcribed genes are soluble heterodisulfide
159 reductase (HdrABC), [NiFe] hydrogenases (groups 3 and 4), ATP synthase, numerous aldehyde
160 ferredoxin oxidoreductase genes, genes for phosphoenolpyruvate (PEP) and pyruvate metabolism,
161 and carbon monoxide dehydrogenase/acetyl CoA synthetase (CODH/ACS). Notably, the Hdr, the
162 group 3 and group 4 hydrogenase (including up to eight NADH-quinone oxidoreductase subunits,
163 e.g., Nuo-like) as well as the ATP synthase are co-encoded in a syntenic block in all of the genomes
164 (**Fig. 4A**). Phylogenetic analysis of the large subunit of group 4 [NiFe]-hydrogenases suggests they
165 are closely related to those of Odinararchaeia, Heimdallarchaeia, and Hermodarchaeia (**Fig. 4B, table**
166 **S8**). However, the exact function of this unclassified Asgard group has not been validated
167 biochemically (26). One clue relies on the identification of eight genes homologous to the
168 hydrophobic subunits of complex I NuoL, M, and N (*E. coli* nomenclature) and Mrp-type Na⁺/H⁺
169 antiporters. Thus, these Asgard archaea may mediate Na⁺/H⁺ translocation coupled to energy
170 generation via ATP synthase (27–29).

171 We employed AlphaFold2 to model the hydrogenase and associated complex I-like
172 modules. Overall, the predicted structure has a cytosolic and membrane-associated portion (**Fig.**
173 **4C**). The cytosolic portion aligned with the respiratory membrane-bound hydrogenase (MBH)
174 from *Pyrococcus furiosus* (27) with high confidence (**Fig. 4D**). When superimposed, the calculated
175 structures of the membrane-associated hydrophobic L, M, K, and S chains aligned to bacterial
176 complex I. In the canonical complex I (30, 31), Chain L, Nqo12, as well as M, N, and K translocate
177 proteins (31, 32), a process that is facilitated by an arm, helix HL that is part of chain L. This helix
178 HL is also present in the L-like subunit of the Asgard complexes (**Fig. 4E**). The helix HL, and the
179 antiporter subunits located between chain L and the subunit that connects to the cytosolic

180 hydrogenase portion, are absent in all characterized respiratory membrane-bound hydrogenases
181 (**Fig. 4E, fig. S7**).

182 The Group 3c cofactor-coupled bidirectional [NiFe] hydrogenase (**fig. S8A**) in
183 combination with HdrABC suggests the capability to bifurcate electrons from H₂ to ferredoxin and
184 an unidentified heterodisulfide compound. This capacity has been observed in methanogenic
185 archaea via the MvhADG–HdrABC system (33, 34). Atabayarchaeia genomes encode two
186 independent gene clusters of the Group 3b NADP-coupled [NiFe] hydrogenases (**fig. S8B**). Their
187 presence suggests the capacity to maintain redox equilibrium and, potentially, grow
188 lithoautotrophically by using H₂ as an electron donor, as suggested for other Asgardarchaeota
189 members (10, 14, 26).

190 Atabayarchaeia and Freyarchaeia encode both the tetrahydromethanopterin (H₄MPT)
191 methyl branch and the carbonyl branch of the Wood–Ljungdahl pathway (WLP) (**fig. S9**). This
192 reversible pathway can be used to reduce CO₂ to acetyl coenzyme A (acetyl CoA), which can be
193 further converted to acetate. This last conversion can lead to energy conservation in both Asgard
194 lineages via substrate-level phosphorylation when mediated by acetate-CoA ligase (see below).
195 We confirmed the expression of almost all of the genes of the methyl and carbonyl branches,
196 including the acetate-CoA ligase, in all complete genomes. When H₂ is present in the ecosystem,
197 these archaea could use the WLP for the reduction of CO₂ or formate and thereby conserving
198 energy. Alternatively, they could use the WLP in reverse to oxidize acetate. In both scenarios, the
199 expression of energy-converting hydrogenases and the ATP synthases suggest a potential role in
200 energy conservation. This involvement may include coupling exergonic electron transfer to
201 establish an ion gradient that fuels the ATP synthase for ATP generation. The metabolic inferences
202 along with the transcriptional data including the expression of *por* genes in all three Asgard
203 genomes, indicates a reliance on an archaeal version of the WLP to perform acetogenesis (34, 35).
204 This acetogenic lifestyle appears to involve energy conservation through a hydrogenase-
205 dependent chemiosmotic mechanism similar to that observed in some acetogenic bacteria (36).

206

207 *Potential for non-methanogenic methylotrophic life-style and carboxydotrophy*

208

209 Despite the absence of the MCR complex, Freyarchaeia genomes have all the necessary genes to
210 synthesize coenzyme-M from sulfopyruvate via the ComABC pathway similar to methanogens
211 (37, 38). Most methanogens conserve energy via the Na⁺-translocating MtrA-H complex, which
212 is encoded by an eight-gene cluster (39). Although Atabayarchaeia and Freyarchaeia do not have
213 the genes for the full complex, Atabayarchaeia-1 has two copies of the CH₃-H₄MPT-dependent
214 methyltransferase subunit A-like (MtrA) and both Freyarchaeia and Atabayarchaeia also encode
215 the CH₃-H₄MPT-dependent methyltransferase subunit H (MtrH), along with a phylogenetically
216 distinct fused polypeptide of MtrA-like and MtrH (**Figure 5A**). Under the conditions prevalent at
217 the time of sampling, the *mtr* genes were only weakly expressed (**table S6, S8**). While the
218 biochemical activity of these divergent non-methanogen-associated MtrA-like and MtrH-like
219 enzymes remain unclear, our phylogenetic analyses suggest they are phylogenetically related to
220 methanogenic MtrA, MtrH, and MtrAH sequences. This suggests their potential role in converting
221 CH₃-H₄MPT to H₄MPT, transferring a methyl group to an acceptor –possibly coenzyme-M, which
222 can be produced by Freyarchaeia–. As they lack the MCR complex, the subsequent fate of the
223 methyl group remains uncertain.

224 Although Atabayarchaeia and Freyarchaeia genomes do not encode MtrE, we identified
225 genes associated with methyltransferase systems encoded in close proximity to the MtrH gene.

226 Specifically, the genomes encode trimethylamine methyltransferase (MttB-like, COG5598
227 superfamily), undefined corrinoid protein (MtbC-like), and putative glycine cleavage system H
228 (gcvH) (**table S9**). Both Atabeyarchaeia and Freyarchaeia genomes encode trimethylamine
229 methyltransferase MttB (COG5598). Phylogenetic analysis suggests that MttB (**fig. S10**) and
230 MtbC (**fig. S11**) belong to a previously uncharacterized group of methyltransferases, similar to
231 those found in Njordarchaeales, Helarchaeales, Odinarchaeia and TACK members, including
232 Brockarchaeia and Thermoproteota. In methanogens that encode *mttB*, this gene has an amber
233 codon encoding the amino acid pyrrolysine in the active site (40, 41). The archaea from this study
234 do not encode pyrrolysine, suggesting Freyarchaeia and Atabeyarchaeia encode a non-pyrrolysine
235 MttB homolog, likely a quaternary amine (QA) dependent methyltransferase (42). Only a fraction
236 of QA methyltransferase substrates have been identified, and these include glycine betaine, proline
237 betaine, carnitine, and butyrobetaine (42–45). The methyl group from the QA may be transferred
238 to THF or H₄MPT branches of the WLP, akin to the mechanisms described in archaea with the
239 capacity for non-methanogenic anaerobic methylotrophy, including Freyarchaeia (Jordarchaeia),
240 Sifarchaeia, Brockarchaeia, and Culexarchaeia (11, 12, 46, 47). Consumption of QA compounds
241 may reduce the pool of potential substrates for methanogenic methane production.
242 We identified genes in the Freyarchaeia genome that potentially encode an aerobic carbon-
243 monoxide dehydrogenase complex (CoxLMS) and associated cofactors. Phylogenetic analysis
244 places the putative CoxL in a monophyletic group with other archaea including
245 Thermoplasmatales, Marsarchaeota, and Culexarchaeia (**fig. S12**). The gene cassette arrangement
246 suggests these archaea may possess the ability to use carbon monoxide as a growth substrate
247 (carboxydrotrophy). However, analysis of the protein sequence reveals that the putative large-
248 subunit aerobic CO dehydrogenases (CoxL) are missing the characteristic VAYRCSFR motif,
249 which is critical for CO binding in the form I Cox proteins (48, 49). Nevertheless, the modeled
250 protein structure, along with the operon organization of the *cox* genes, points to a novel type of
251 Cox system in archaea (**fig. S13**). Alternatively, it is possible that this complex enables the
252 utilization of alternative substrates, such as aldehydes or purines, as a member of the aldehyde
253 oxidase superfamily (47, 49, 50).

254

255

256 *Carbon compound metabolic pathways*

257

258 There are indications that Freyarchaeia and Atabeyarchaeia display distinct metabolic
259 preferences for various soil carbon compounds (**Fig. 2;fig. S13**). Freyarchaeia exhibit a genetic
260 repertoire to break down various extracellular lignin-derived compounds including 5-
261 carboxyvanillate. Other substrates that we predict can be metabolized by Freyarchaeia
262 carbohydrate-active enzymes include hemicellulose (C5), cellobiose, maltose, and cellulose (C12).
263 We predict that cellodextrin (C18) compounds can be converted to glucose via beta-glucosidase
264 (BglBX). The findings implicate Freyarchaeia in the metabolism of plant-derived soil carbon
265 compounds. Glucose, resulting from the degradation of complex carbohydrates, as well as ribulose
266 and other carbon substrates, likely enters the modified Embden-Meyerhof-Parnas (EMP) pathway,
267 yet the genes of this EMP pathway genes are only weakly expressed (**fig. S14, table S6, S8**).
268 Additionally, Freyarchaeia encode and express an array of genes for the uptake of carbohydrates
269 including major facilitator superfamily sugar transporters and ABC-sugar transporters suggesting
270 an active role in efficiently assimilating diverse carbon substrates from soil environments
271 Atabeyarchaeia also harbor genes of the EMP glycolytic pathway, producing ATP through the

272 conversion of acetyl-CoA to acetate (**fig. S13**). Unlike Freyarchaeia which likely feed glucose into
273 the EMP pathway, the entry point for Atabeyarchaeia to the EMP pathway appears to be fructose
274 6-phosphate (F6P). This is relatively uncommon for Asgard archaea but is reminiscent of the
275 pathway in Helarchaeales (7), an order of Lokiarchaeia. We identified Atabeyarchaeia transcripts
276 for all but one of the genes for the steps from G6P to acetate (table S8).

277 Atabeyarchaeia and Freyarchaeia utilize different enzymes to produce pyruvate.
278 Atabeyarchaeia encode the oxygen-sensitive reversible enzyme, pyruvate:phosphate dikinase
279 (PpdK); whereas Freyarchaeia encodes unidirectional pyruvate water
280 dikinase/phosphoenolpyruvate synthase (PpS) and pyruvate kinase (Pk), producing
281 phosphoenolpyruvate and pyruvate (51), respectively. Pyruvate generated via EMP pathway can
282 be then converted to acetyl-CoA by pyruvate:ferredoxin oxidoreductase (PorABCDG) complex
283 using a low-potential electron carrier such as a ferredoxin as the electron donor. Alternatively,
284 acetyl-CoA can also be generated via pyruvate formate-lyase (pflD) generating formate as a
285 byproduct. The final step involves the conversion of acetyl-CoA to acetate via acetate-CoA ligase
286 (ADP-forming) producing ATP via substrate level phosphorylation- a crucial energy conserving
287 step during fermentation of carbon compounds in both lineages.

288 Lacking the ability to phosphorylate C6 carbon sources, Atabeyarchaeia converts ribulose-
289 5-phosphate (C5) and fixes formaldehyde (C1) into hexulose-6-phosphate (H6P) via the ribulose
290 monophosphate (RuMP) and non-oxidative pentose phosphate (NO-PPP) pathways (**Fig.2, fig.**
291 **S14**). The Atabeyarchaeia RuMP pathway bifunctional enzymes (HPS-PH and Fae-HPS) are
292 common in archaea and similar to methylotrophic bacterial homologs (52). The RuMP pathway in
293 these Asgard archaea can modulate the formaldehyde availability, a byproduct of methanol
294 oxidation, microbial organic matter decomposition, and combustion. High expression of aldehyde-
295 ferredoxin oxidoreductases (AOR) genes suggest another mechanism for the interconversion of
296 organic acids to aldehydes. For example, aldehyde detoxification (e.g., formaldehyde to formate)
297 and source of acetate from acetaldehyde Atabeyarchaeia-1, Atabeyarchaeia-2, and Freyarchaeia
298 encode multiple AOR gene copies 5, 6, and 8 respectively. Phylogenetic analyses (**fig. S15**)
299 suggest that both Asgard lineages encode AOR genes related to the FOR family that oxidize C1-
300 C3 aldehydes or aliphatic and aromatic aldehydes (e.g. formaldehyde or glyceraldehyde) (53–55).
301 Furthermore, Freyarchaeia also encodes a tungsten-based AOR-type enzyme (XOR family) found
302 in cellulolytic anaerobes with undefined substrate specificity (56) (**fig. S15**). Of the classified
303 AORs, only one gene is expressed in Atabeyarchaeia-2 (**Figure 3**). Yet, some of the unclassified
304 AOR genes are among the most highly expressed genes in the Atabeyarchaeia genomes. Despite
305 the lack of biochemical characterization for most AOR families, these observations suggest a key
306 role of multiple aldehydes in the generation of reducing power in the form of reduced ferredoxin.

307 Similar to other Asgard archaea (7, 10, 26), Atabeyarchaeia and Freyarchaeia encode genes
308 for the large subunit of type IV and methanogenic type III Ribulose 1,5-bisphosphate carboxylase
309 (RbcL) (**fig. S16**) a key enzyme in the partial nucleotide salvage pathway. This pathway facilitates
310 the conversion of adenosine monophosphate (AMP) to 3-phosphoglycerate (3-PG), potentially
311 leading to further metabolism into acetyl-CoA (57).

312 Anaerobic glycerol (C3) metabolism by Atabeyarchaeia and Freyarchaeia is predicted
313 based on the presence of glycerol kinase (GlpK), which forms glycerol-3-phosphate (3PG) from
314 glycerol. 3PG (along with F6P) can be broken down via the EMP pathway or 3PG can be converted
315 to dihydroxyacetone phosphate (DHAP) via GlpABC. DHAP can also serve as a precursor for sn-
316 glycerol-1-phosphate (G1P), the backbone of archaeal phospholipids. Freyarchaeia have an extra

317 GlpABC operon, the GlpA subunit of which clusters phylogenetically with GlpA of
318 Halobacteriales, the only known archaeal group capable of glycerol assimilation (**fig. S17**).

319 All three genomes have a partial TCA cycle similar to other anaerobic archaeal groups such
320 as methanogens (58). They encode succinate dehydrogenase, succinyl-CoA synthetase, 2-
321 oxoglutarate ferredoxin reductase that are important intermediates for amino acid degradation
322 (e.g., glutamate). Only Atabayarchaeia can convert fumarate to malate via fumarate hydratase. The
323 only portion of TCA cycle transcribed in any genome is 2-oxoglutarate/2-oxoacid ferredoxin
324 oxidoreductase, which can produce reducing power in the form of NADH.

325 A clue suggesting that amino acids are an important resource for Atabayarchaeia and
326 Freyarchaeia is the high expression of genes for protein and peptide breakdown (**Figure 2**). All
327 three organisms are predicted to have the capacity to break down fatty acids via beta oxidation
328 including crotonate (short-chain fatty acid) via the poorly described crotonate pathway.
329 Furthermore they encode some enzymes involved in fermenting amino acids to H⁺, ammonium,
330 acetate, and NAD(P)H via the hydroxyglutarate pathway (**table S7**). The genomes also encode
331 amino acid transporters and these are also highly transcribed in both archaeal groups. The ability
332 to anaerobically degrade amino acids is consistent with predictions of the metabolism of the last
333 Asgard common ancestor (4, 9).

334 Additionally, Freyarchaeia and Atabayarchaeia can reverse the step in the formyl branch
335 of the WLP that transforms glycine into methylenetetrahydrofolate (methylene-THF). Methylene-
336 THF may then be converted to methyl-THF and then to formyl-THF, producing reducing power
337 (**Figure 2**). Ultimately, the methyl group may be used to form acetate via the WLP. Interestingly
338 Atabayarchaeia-2 and Freyarchaeia expressed methylenetetrahydrofolate reductase (MTHFR) that
339 is homologous to the enzyme used in the bacterial WLP and also plays a role in folate biosynthesis.
340

341 *Environmental protection and adaptations*

342
343 We predict that Atabayarchaeia and Freyarchaeia are anaerobes expressing genes that
344 encode oxygen-sensitive enzymes and proteins that protect against oxidative and other
345 environmental stressors. Interestingly, all three organisms encode an ancestral version of clade I
346 catalases (KatE) (**fig. S18**), Fe-Mn superoxide dismutase (SOD2), and unique to Freyarchaeia, a
347 catalase-peroxidase (**fig. S19**) for protection against reactive oxygen species (ROS) (**fig. S20**).
348 Previous analyses have described these expressed enzymes in acetogenic and sulfate-reducing
349 bacteria and methanogenic archaea, but to our knowledge, not in Asgard archaea, indicating a
350 potential adaptation to soil environments(59). We also identified transcription for other
351 environmental and stress responses, including transporters (e.g., nickel, arsenite, magnesium, iron,
352 and copper), and heat shock proteins.
353

354 We infer that Atabayarchaeia and Freyarchaeia use selenocysteine (Sec), the 21st amino
355 acid, due to the presence of the Sec-specific elongation factor and Sec tRNA in their genomes.
356 Additional Sec components, including phosphoseryl-tRNA kinase (Pstk), Sec synthase (SecS),
357 selenophosphate synthetase (SPS) genes, and multiple Eukaryotic-like Sec Insertion Sequences
358 are also present (**table S10**). Phylogenetic analysis shows that the Sec elongation factor sequences
359 from Atabayarchaeia and Freyarchaeia are closely related to other Asgard members and
360 Eukaryotes (**fig. S21**). We identified multiple selenoproteins encoded within each genome,
361 including CoB-CoM heterodisulfide reductase iron-sulfur subunit (HdrA), peroxiredoxin family
362 protein (Prx-like), selenophosphate synthetase (SPS), and the small subunit (~50 aa) of NiFeSec

363 (VhuU). In VhuU, Sec plays a crucial role in mitigating oxidative stress (55). Sec can also enhance
364 the catalytic efficiency of redox proteins (56, 58), and the identified selenoproteins have the
365 characteristic CXXU or UXXC sequence (**table S11**) observed in redox-active motifs (57).

366 367 **Discussion**

368
369 Here, we reconstructed and validated three complete Asgard archaeal genomes from wetland soils
370 in which these archaea comprise less than 1% of complex microbial communities. We used these
371 genomes to define their chromosome lengths, structure and replication modes. It is relatively
372 common for authors to report circularized genomes as complete, but this may be erroneous due to
373 the prominence of local assembly errors, chimeras, scaffolding gaps and other issues in de novo
374 metagenome assemblies (21, 60). Our genomes were thoroughly inspected, corrected and vetted
375 after circularization, steps previously described to complete genomes from metagenomes (61).
376 These complete genomes are one of the first manual curations of short-read metagenomic data
377 verified entirely with long-read analysis (Oxford Nanopore and/or PacBio) and the first complete
378 short-read environmental Asgard genomes. Two of these genomes are from Atabeyarchaeia, a
379 previously undescribed Asgard group and the first complete genome for Freyarchaeia. We predict
380 bidirectional replication in Freyarchaeia and Atabeyarchaeia, suggesting bidirectional replication
381 could have been present in the last common ancestor of eukaryotes and archaea, potentially playing
382 a role in the emergence of the complex cellular organization characteristic of eukaryotes.

383
384 Overall, prior studies predict that Asgard archaea degrade proteins, carbohydrates, fatty
385 acids, amino acids, and hydrocarbons (5, 6, 10, 62). Lokiarchaeales, Thorarchaeia, Odinararchaeia,
386 and Heimdallarchaeia are primarily organoheterotrophs with varying capacities to consume and
387 produce hydrogen (26). Helarchaeales are proposed to anaerobically oxidize hydrocarbons (7, 10,
388 63), whereas Freyarchaeia and Sifarchaeia are predicted to be heterorganotrophic acetogens
389 capable of utilizing methylated amines (11, 12). Hermodarchaeia are proposed to degrade alkanes
390 and aromatic compounds via the alkyl/benzyl-succinate synthase and benzoyl-CoA pathway (10).
391 Gerdarchaeales may be facultative anaerobes and utilize both organic and inorganic carbon (8).
392 Atabeyarchaeia and Freyarchaeia share several metabolic pathways with new lineages from the
393 Asgard sister-clade TACK (e.g., Brock- and Culexarchaeia) and other deeply branching Asgard
394 lineages. Based on the genomic and metatranscriptomic analyses, we predict that the soil-
395 associated Atabeyarchaeia and Freyarchaeia are chemoheterotrophs that likely degrade amino
396 acids and other carbon compounds. Both encode the EMP Pathway for cellular respiration and the
397 WLP for CO₂ fixation.

398 Although Atabeyarchaeia and Freyarchaeia share key central metabolic pathways, they
399 differ in that Freyarchaeia can metabolize compounds such as formaldehyde (C1), glycerol (C3),
400 ribulose (C5), and glucose (C6), whereas, Atabeyarchaeia can only metabolize C1, C3 and C5
401 compounds (**Fig. 2**). The ability to metabolize C3 and C5 compounds is rare in Asgard archaea.
402 While the entry points into the EMP pathway differ between the two, both exhibit the genetic
403 repertoire necessary for converting carbohydrates into acetate. Both Atabeyarchaeia and
404 Freyarchaeia may also be capable of growth as anaerobic acetogens via acetate production through
405 the WLP. Similar to other Asgard archaea, they have methyltransferase complexes involved in the
406 catabolism of quaternary amines (or yet unknown methylated substrates). Through the use of
407 methylated compounds, they may compete with methanogens and other anaerobic methylotrophic
408 groups that rely on these substrates for methane production. These results align with recent studies

409 suggesting a broader presence of methylotrophic metabolisms among archaea (10, 46, 47). It also
410 opens up avenues for exploring the environmental impact of these metabolisms, particularly in
411 relation to carbon cycling and greenhouse gas emissions (64).

412 Of particular interest is the predicted metabolic capability of Atabayarchaeia and
413 Freyarchaeia to degrade aldehydes. Aldehydes in soils come from several sources, including the
414 microbial breakdown of methanol potentially produced from methane oxidation, degradation of
415 plant and animal compounds, and products of industrial combustion and wildfires (e.g., volatile
416 organic compounds). In fact, the California wetland soil that hosts these archaea contain charcoal,
417 likely produced by wildfires. They are also predicted to be capable of growing on glycerol under
418 anaerobic conditions capacity previously undescribed in Asgard archaea. Glycerol may be present
419 in soil by the lysis of bacteria, yeast, and methanogenic archaeal cells that use glycerol as a solute,
420 or by microbial fermentation of plant and animal triglycerides and phospholipids(65). The
421 presence of glycerol kinase and the respiratory glycerol-3-phosphate dehydrogenase (GlpABC) in
422 Atabayarchaeia and Freyarchaeia indicates these archaea might use with glycerol or glycerol-3-
423 phosphate and fumarate as the terminal electron acceptor associated with proton translocation.
424 This finding suggests a broader role for glycerol in Asgard archaeal energy metabolism and points
425 to a possible conservation of this mechanism across different anaerobic environments.
426 Understanding how these archaea metabolize glycerol will enhance our knowledge of their
427 ecological roles and contributions to the carbon cycle in wetland ecosystems. Atabayarchaeia and
428 Freyarchaeia also produce and consume small organic molecules and H₂ that serve as substrates
429 for methane production by methanogens that coexist in wetland soil.

430 The soil Asgard archaea encodes group 3c [NiFe]-hydrogenase genes, which were shown
431 to be highly expressed *in situ*. Under specific conditions, autotrophic growth is likely supported
432 by H₂ oxidation via the WLP. The presence of syntenic blocks encoding heterodisulfide reductase
433 complexes, [NiFe] hydrogenases, and ATP synthase suggests a sophisticated apparatus for energy
434 transduction, resembling mechanisms previously characterized in other archaeal groups (34).
435 Additionally, our results suggest the existence of an electron bifurcation mechanism in both
436 Asgard archaea lineages, where electrons can be transferred from H₂ to ferredoxin and an
437 unidentified heterodisulfide intermediate (26). Atabayarchaeia and Freyarchaeia also have
438 membrane-bound group 4 [NiFe]-hydrogenases that likely facilitate the oxidation of reduced
439 ferredoxin generated through fermentative metabolism. However, this complex is novel in that it
440 includes a HL helix on the L-like subunit and two antiporters, neither of which are part of
441 biochemically characterized group 4 respiratory hydrogenases. The functional modeling of these
442 complexes reveals structural congruences with known respiratory enzymes, hinting at a potential
443 for chemiosmotic energy conservation that may be a widespread feature among the Asgard clade.
444 The findings indicate a potential evolutionary connection between hydrogenases and complex I,
445 aligning with the hypothesis that complex I may have evolved from ancestral hydrogenases (30,
446 66).

447 These complete genomes provide insight into the unique metabolic pathways of Asgard
448 archaea in soil environments, previously missed in primarily sediment-based descriptions. Of
449 particular interest is the identification of genes encoding enzymes for oxidative stress response in
450 both Atabayarchaeia and Freyarchaeia, despite their anaerobic nature. The use of selenocysteine
451 in key enzymes may provide another mechanism for dealing with increased oxidative stress. These
452 Asgardarchaeota genomes suggest an adaptation to transient oxidative conditions in soil
453 environments and additional competition for methanogenesis and anaerobic methylotrophy
454 substrates.

455

456 **Conclusions**

457

458 We manually curated three complete genomes for Asgard archaea from wetland soils, uncovering
459 bidirectional replication and an unexpected abundance of introns in tRNA genes. These features
460 suggest another facet of the evolutionary relationship between archaea and eukaryotes. Metabolic
461 reconstruction and metatranscriptomic measurements of *in situ* activity revealed a non-
462 methanogenic, acetogenic lifestyle and a diverse array of proteins likely involved in energy
463 conservation. The findings point to metabolic flexibility and adaptation to the dynamic soil
464 conditions of wetlands. Finally, they contribute to cycling of carbon compounds that are relevant
465 for methane production by coexisting methanogenic archaea.

466

467 **References:**

- 468 1. A. Spang, J. H. Saw, S. L. Jørgensen, K. Zaremba-Niedzwiedzka, J. Martijn, A. E. Lind, R.
469 van Eijk, C. Schleper, L. Guy, T. J. G. Ettema, Complex archaea that bridge the gap
470 between prokaryotes and eukaryotes. *Nature*. **521**, 173–179 (2015).
- 471 2. K. Zaremba-Niedzwiedzka, E. F. Caceres, J. H. Saw, D. Bäckström, L. Juzokaite, E.
472 Vancaester, K. W. Seitz, K. Anantharaman, P. Starnawski, K. U. Kjeldsen, M. B. Stott, T.
473 Nunoura, J. F. Banfield, A. Schramm, B. J. Baker, A. Spang, T. J. G. Ettema, Asgard
474 archaea illuminate the origin of eukaryotic cellular complexity. *Nature*. **541**, 353–358
475 (2017).
- 476 3. Y. Liu, K. S. Makarova, W.-C. Huang, Y. I. Wolf, A. N. Nikolskaya, X. Zhang, M. Cai, C.-
477 J. Zhang, W. Xu, Z. Luo, L. Cheng, E. V. Koonin, M. Li, Expanded diversity of Asgard
478 archaea and their relationships with eukaryotes. *Nature*. **593**, 553–557 (2021).
- 479 4. L. Eme, D. Tamarit, E. F. Caceres, C. W. Stairs, V. De Anda, M. E. Schön, K. W. Seitz, N.
480 Dombrowski, W. H. Lewis, F. Homa, J. H. Saw, J. Lombard, T. Nunoura, W.-J. Li, Z.-S.
481 Hua, L.-X. Chen, J. F. Banfield, E. S. John, A.-L. Reysenbach, M. B. Stott, A. Schramm, K.
482 U. Kjeldsen, A. P. Teske, B. J. Baker, T. J. G. Ettema, Inference and reconstruction of the
483 heimdallarchaeial ancestry of eukaryotes. *Nature*. **618**, 992–999 (2023).
- 484 5. K. W. Seitz, C. S. Lazar, K.-U. Hinrichs, A. P. Teske, B. J. Baker, Genomic reconstruction
485 of a novel, deeply branched sediment archaeal phylum with pathways for acetogenesis and
486 sulfur reduction. *ISME J.* **10**, 1696–1705 (2016).
- 487 6. Y. Liu, Z. Zhou, J. Pan, B. J. Baker, J.-D. Gu, M. Li, Comparative genomic inference
488 suggests mixotrophic lifestyle for Thorarchaeota. *ISME J.* **12**, 1021–1031 (2018).
- 489 7. K. W. Seitz, N. Dombrowski, L. Eme, A. Spang, J. Lombard, J. R. Sieber, A. P. Teske, T. J.
490 G. Ettema, B. J. Baker, Asgard archaea capable of anaerobic hydrocarbon cycling. *Nat.*
491 *Commun.* **10**, 1822 (2019).
- 492 8. M. Cai, Y. Liu, X. Yin, Z. Zhou, M. W. Friedrich, T. Richter-Heitmman, R. Nimzyk, A.
493 Kulkarni, X. Wang, W. Li, J. Pan, Y. Yang, J.-D. Gu, M. Li, Diverse Asgard archaea
494 including the novel phylum Gerdarchaeota participate in organic matter degradation. *Sci.*

- 495 *China Life Sci.* **63**, 886–897 (2020).
- 496 9. H. Imachi, M. K. Nobu, N. Nakahara, Y. Morono, M. Ogawara, Y. Takaki, Y. Takano, K.
497 Uematsu, T. Ikuta, M. Ito, Y. Matsui, M. Miyazaki, K. Murata, Y. Saito, S. Sakai, C. Song,
498 E. Tasumi, Y. Yamanaka, T. Yamaguchi, Y. Kamagata, H. Tamaki, K. Takai, Isolation of
499 an archaeon at the prokaryote-eukaryote interface. *Nature*. **577**, 519–525 (2020).
- 500 10. J.-W. Zhang, H.-P. Dong, L.-J. Hou, Y. Liu, Y.-F. Ou, Y.-L. Zheng, P. Han, X. Liang, G.-
501 Y. Yin, D.-M. Wu, M. Liu, M. Li, Newly discovered Asgard archaea Hermodarchaeota
502 potentially degrade alkanes and aromatics via alkyl/benzyl-succinate synthase and benzoyl-
503 CoA pathway. *ISME J.* **15**, 1826–1843 (2021).
- 504 11. Farag Ibrahim F., Zhao Rui, Biddle Jennifer F., “Sifarchaeota,” a Novel Asgard Phylum
505 from Costa Rican Sediment Capable of Polysaccharide Degradation and Anaerobic
506 Methylothy. *Appl. Environ. Microbiol.* **87**, e02584–20 (2021).
- 507 12. J. Sun, P. N. Evans, E. J. Gagen, B. J. Woodcroft, B. P. Hedlund, T. Woyke, P. Hugenholtz,
508 C. Rinke, Recoding of stop codons expands the metabolic potential of two novel
509 Asgardarchaeota lineages. *ISME Commun.* **1**, 30 (2021).
- 510 13. M. Cai, T. Richter-Heitmann, X. Yin, W.-C. Huang, Y. Yang, C. Zhang, C. Duan, J. Pan, Y.
511 Liu, Y. Liu, M. W. Friedrich, M. Li, Ecological features and global distribution of Asgard
512 archaea. *Sci. Total Environ.* **758**, 143581 (2021).
- 513 14. R. Xie, Y. Wang, D. Huang, J. Hou, L. Li, H. Hu, X. Zhao, F. Wang, Expanding Asgard
514 members in the domain of Archaea sheds new light on the origin of eukaryotes. *Sci. China*
515 *Life Sci.* **65**, 818–829 (2022).
- 516 15. T. Rodrigues-Oliveira, F. Wollweber, R. I. Ponce-Toledo, J. Xu, S. K.-M. R. Rittmann, A.
517 Klingl, M. Pilhofer, C. Schleper, Actin cytoskeleton and complex cell architecture in an
518 Asgard archaeon. *Nature*. **613**, 332–339 (2023).
- 519 16. D. Tamarit, E. F. Caceres, M. Krupovic, R. Nijland, L. Eme, N. P. Robinson, T. J. G.
520 Ettema, A closed Candidatus Odinarchaeum chromosome exposes Asgard archaeal viruses.
521 *Nat Microbiol.* **7**, 948–952 (2022).
- 522 17. F. Wu, D. R. Speth, A. Philosofo, A. Crémière, A. Narayanan, R. A. Barco, S. A. Connon, J.
523 P. Amend, I. A. Antoshechkin, V. J. Orphan, Unique mobile elements and scalable gene
524 flow at the prokaryote-eukaryote boundary revealed by circularized Asgard archaea
525 genomes. *Nat Microbiol.* **7**, 200–212 (2022).
- 526 18. J. Sun, P. N. Evans, E. J. Gagen, B. J. Woodcroft, B. P. Hedlund, T. Woyke, P. Hugenholtz,
527 C. Rinke, Correction: Recoding of stop codons expands the metabolic potential of two
528 novel Asgardarchaeota. *ISME Communications.* **2**, 1–1 (2022).
- 529 19. B. Al-Shayeb, R. Sachdeva, L.-X. Chen, F. Ward, P. Munk, A. Devoto, C. J. Castelle, M. R.
530 Olm, K. Bouma-Gregson, Y. Amano, C. He, R. Méheust, B. Brooks, A. Thomas, A. Lavy,
531 P. Matheus-Carnevali, C. Sun, D. S. A. Goltsman, M. A. Borton, A. Sharrar, A. L. Jaffe, T.

- 532 C. Nelson, R. Kantor, R. Keren, K. R. Lane, I. F. Farag, S. Lei, K. Finstad, R. Amundson,
533 K. Anantharaman, J. Zhou, A. J. Probst, M. E. Power, S. G. Tringe, W.-J. Li, K. Wrighton,
534 S. Harrison, M. Morowitz, D. A. Relman, J. A. Doudna, A.-C. Lehours, L. Warren, J. H. D.
535 Cate, J. M. Santini, J. F. Banfield, Clades of huge phages from across Earth's ecosystems.
536 *Nature*. **578**, 425–431 (2020).
- 537 20. B. Al-Shayeb, M. C. Schoelmerich, J. West-Roberts, L. E. Valentin-Alvarado, R. Sachdeva,
538 S. Mullen, A. Crits-Christoph, M. J. Wilkins, K. H. Williams, J. A. Doudna, J. F. Banfield,
539 Borgs are giant genetic elements with potential to expand metabolic capacity. *Nature*. **610**,
540 731–736 (2022).
- 541 21. L.-X. Chen, K. Anantharaman, A. Shaiber, A. M. Eren, J. F. Banfield, Accurate and
542 complete genomes from metagenomes. *Genome Res.* **30**, 315–333 (2020).
- 543 22. C. Marck, H. Grosjean, Identification of BHB splicing motifs in intron-containing tRNAs
544 from 18 archaea: evolutionary implications. *RNA*. **9**, 1516–1531 (2003).
- 545 23. J. Sugahara, K. Kikuta, K. Fujishima, N. Yachie, M. Tomita, A. Kanai, Comprehensive
546 analysis of archaeal tRNA genes reveals rapid increase of tRNA introns in the order
547 thermoproteales. *Mol. Biol. Evol.* **25**, 2709–2716 (2008).
- 548 24. G. D. Tocchini-Valentini, P. Fruscoloni, G. P. Tocchini-Valentini, Evolution of introns in
549 the archaeal world. *Proc. Natl. Acad. Sci. U. S. A.* **108**, 4782–4787 (2011).
- 550 25. T. Yoshihisa, Handling tRNA introns, archaeal way and eukaryotic way. *Front. Genet.* **5**,
551 213 (2014).
- 552 26. A. Spang, C. W. Stairs, N. Dombrowski, L. Eme, J. Lombard, E. F. Caceres, C. Greening,
553 B. J. Baker, T. J. G. Ettema, Proposal of the reverse flow model for the origin of the
554 eukaryotic cell based on comparative analyses of Asgard archaeal metabolism. *Nat*
555 *Microbiol.* **4**, 1138–1148 (2019).
- 556 27. H. Yu, C.-H. Wu, G. J. Schut, D. K. Haja, G. Zhao, J. W. Peters, M. W. W. Adams, H. Li,
557 Structure of an Ancient Respiratory System. *Cell*. **173**, 1636–1649.e16 (2018).
- 558 28. B. C. Marreiros, A. P. Batista, A. M. S. Duarte, M. M. Pereira, A missing link between
559 complex I and group 4 membrane-bound [NiFe] hydrogenases. *Biochim. Biophys. Acta.*
560 **1827**, 198–209 (2013).
- 561 29. R. G. Efremov, L. A. Sazanov, The coupling mechanism of respiratory complex I - a
562 structural and evolutionary perspective. *Biochim. Biophys. Acta.* **1817**, 1785–1795 (2012).
- 563 30. R. G. Efremov, L. A. Sazanov, Structure of the membrane domain of respiratory complex I.
564 *Nature*. **476**, 414–420 (2011).
- 565 31. R. Baradaran, J. M. Berrisford, G. S. Minhas, L. A. Sazanov, Crystal structure of the entire
566 respiratory complex I. *Nature*. **494**, 443–448 (2013).

- 567 32. E. Nakamaru-Ogiso, M.-C. Kao, H. Chen, S. C. Sinha, T. Yagi, T. Ohnishi, The membrane
568 subunit NuoL(ND5) is involved in the indirect proton pumping mechanism of Escherichia
569 coli complex I. *J. Biol. Chem.* **285**, 39070–39078 (2010).
- 570 33. W. Buckel, R. K. Thauer, Energy conservation via electron bifurcating ferredoxin reduction
571 and proton/Na(+) translocating ferredoxin oxidation. *Biochim. Biophys. Acta.* **1827**, 94–113
572 (2013).
- 573 34. F. L. Sousa, S. Neukirchen, J. F. Allen, N. Lane, W. F. Martin, Lokiarchaeon is hydrogen
574 dependent. *Nat Microbiol.* **1**, 16034 (2016).
- 575 35. W. D. Orsi, A. Vuillemin, P. Rodriguez, Ö. K. Coskun, G. V. Gomez-Saez, G. Lavik, V.
576 Mohrholz, T. G. Ferdelman, Metabolic activity analyses demonstrate that Lokiarchaeon
577 exhibits homoacetogenesis in sulfidic marine sediments. *Nat Microbiol.* **5**, 248–255 (2020).
- 578 36. M. C. Schoelmerich, V. Müller, Energy conservation by a hydrogenase-dependent
579 chemiosmotic mechanism in an ancient metabolic pathway. *Proc. Natl. Acad. Sci. U. S. A.*
580 **116**, 6329–6334 (2019).
- 581 37. D. E. Graham, R. H. White, Elucidation of methanogenic coenzyme biosyntheses: from
582 spectroscopy to genomics. *Nat. Prod. Rep.* **19**, 133–147 (2002).
- 583 38. R. H. White, Biosynthesis of coenzyme M (2-mercaptoethanesulfonic acid). *Biochemistry.*
584 **24**, 6487–6493 (1985).
- 585 39. G. Gottschalk, R. K. Thauer, The Na(+)-translocating methyltransferase complex from
586 methanogenic archaea. *Biochim. Biophys. Acta.* **1505**, 28–36 (2001).
- 587 40. B. Hao, W. Gong, T. K. Ferguson, C. M. James, J. A. Krzycki, M. K. Chan, A new UAG-
588 encoded residue in the structure of a methanogen methyltransferase. *Science.* **296**, 1462–
589 1466 (2002).
- 590 41. J. Li, P. T. Kang, R. Jiang, J. Y. Lee, J. A. Soares, J. A. Krzycki, M. K. Chan, Insights into
591 pyrrolysine function from structures of a trimethylamine methyltransferase and its corrinoid
592 protein complex. *Commun Biol.* **6**, 54 (2023).
- 593 42. T. Ticak, D. J. Kountz, K. E. Gerosky, J. A. Krzycki, D. J. Ferguson Jr, A nonpyrrolysine
594 member of the widely distributed trimethylamine methyltransferase family is a glycine
595 betaine methyltransferase. *Proc. Natl. Acad. Sci. U. S. A.* **111**, E4668–76 (2014).
- 596 43. J. W. Picking, E. J. Behrman, L. Zhang, J. A. Krzycki, MtpB, a member of the MttB
597 superfamily from the human intestinal acetogen *Eubacterium limosum*, catalyzes proline
598 betaine demethylation. *J. Biol. Chem.* **294**, 13697–13707 (2019).
- 599 44. D. J. Kountz, E. J. Behrman, L. Zhang, J. A. Krzycki, MtcB, a member of the MttB
600 superfamily from the human gut acetogen *Eubacterium limosum*, is a cobalamin-dependent
601 carnitine demethylase. *Journal of Biological* (2020) (available at
602 [https://www.jbc.org/article/S0021-9258\(17\)50060-5/abstract](https://www.jbc.org/article/S0021-9258(17)50060-5/abstract)).

- 603 45. J. B. Ellenbogen, R. Jiang, D. J. Kountz, L. Zhang, J. A. Krzycki, The MttB superfamily
604 member MtyB from the human gut symbiont *Eubacterium limosum* is a cobalamin-
605 dependent γ -butyrobetaine methyltransferase. *J. Biol. Chem.* **297**, 101327 (2021).
- 606 46. V. De Anda, L.-X. Chen, N. Dombrowski, Z.-S. Hua, H.-C. Jiang, J. F. Banfield, W.-J. Li,
607 B. J. Baker, Brockarchaeota, a novel archaeal phylum with unique and versatile carbon
608 cycling pathways. *Nat. Commun.* **12**, 2404 (2021).
- 609 47. A. J. Kohtz, Z. J. Jay, M. M. Lynes, V. Krukenberg, R. Hatzenpichler, Culexarchaeia, a
610 novel archaeal class of anaerobic generalists inhabiting geothermal environments. *ISME*
611 *Communications*. **2**, 1–13 (2022).
- 612 48. H. Dobbek, L. Gremer, R. Kiefersauer, R. Huber, O. Meyer, Catalysis at a dinuclear
613 [CuSMo(O)OH] cluster in a CO dehydrogenase resolved at 1.1-Å resolution. *Proceedings*
614 *of the National Academy of Sciences*. **99**, 15971–15976 (2002).
- 615 49. P. R. F. Cordero, K. Bayly, P. Man Leung, C. Huang, Z. F. Islam, R. B. Schittenhelm, G.
616 M. King, C. Greening, Atmospheric carbon monoxide oxidation is a widespread mechanism
617 supporting microbial survival. *ISME J.* **13**, 2868–2881 (2019).
- 618 50. J. P. Beam, Z. J. Jay, M. C. Schmid, D. B. Rusch, M. F. Romine, R. de M. Jennings, M. A.
619 Kozubal, S. G. Tringe, M. Wagner, W. P. Inskeep, Ecophysiology of an uncultivated
620 lineage of Aigarchaeota from an oxic, hot spring filamentous “streamer” community. *ISME*
621 *J.* **10**, 210–224 (2016).
- 622 51. C. Bräsen, D. Esser, B. Rauch, B. Siebers, Carbohydrate metabolism in Archaea: current
623 insights into unusual enzymes and pathways and their regulation. *Microbiol. Mol. Biol. Rev.*
624 **78**, 89–175 (2014).
- 625 52. N. Kato, H. Yurimoto, R. K. Thauer, The physiological role of the ribulose monophosphate
626 pathway in bacteria and archaea. *Biosci. Biotechnol. Biochem.* **70**, 10–21 (2006).
- 627 53. F. Arndt, G. Schmitt, A. Winiarska, M. Saft, A. Seubert, J. Kahnt, J. Heider,
628 Characterization of an Aldehyde Oxidoreductase From the Mesophilic Bacterium
629 *Aromatoleum aromaticum* EbN1, a Member of a New Subfamily of Tungsten-Containing
630 Enzymes. *Front. Microbiol.* **10**, 71 (2019).
- 631 54. S. Mukund, M. W. Adams, Glyceraldehyde-3-phosphate ferredoxin oxidoreductase, a novel
632 tungsten-containing enzyme with a potential glycolytic role in the hyperthermophilic
633 archaeon *Pyrococcus furiosus*. *J. Biol. Chem.* **270**, 8389–8392 (1995).
- 634 55. L. E. Bevers, E. Bol, P.-L. Hagedoorn, W. R. Hagen, WOR5, a novel tungsten-containing
635 aldehyde oxidoreductase from *Pyrococcus furiosus* with a broad substrate Specificity. *J.*
636 *Bacteriol.* **187**, 7056–7061 (2005).
- 637 56. I. M. Scott, G. M. Rubinstein, G. L. Lipscomb, M. Basen, G. J. Schut, A. M. Rhaesa, W. A.
638 Lancaster, F. L. Poole 2nd, R. M. Kelly, M. W. W. Adams, A New Class of Tungsten-
639 Containing Oxidoreductase in *Caldicellulosiruptor*, a Genus of Plant Biomass-Degrading

- 640 Thermophilic Bacteria. *Appl. Environ. Microbiol.* **81**, 7339–7347 (2015).
- 641 57. F. R. Tabita, S. Satagopan, T. E. Hanson, N. E. Kreel, S. S. Scott, Distinct form I, II, III,
642 and IV Rubisco proteins from the three kingdoms of life provide clues about Rubisco
643 evolution and structure/function relationships. *J. Exp. Bot.* **59**, 1515–1524 (2008).
- 644 58. K. Lang, J. Schuldes, A. Klingl, A. Poehlein, R. Daniel, A. Brunea, New mode of energy
645 metabolism in the seventh order of methanogens as revealed by comparative genome
646 analysis of “Candidatus methanoplasma termitum.” *Appl. Environ. Microbiol.* **81**, 1338–
647 1352 (2015).
- 648 59. A. L. Brioukhanov, A. I. Netrusov, Catalase and superoxide dismutase: distribution,
649 properties, and physiological role in cells of strict anaerobes. *Biochemistry* . **69**, 949–962
650 (2004).
- 651 60. M. Watson, A. Warr, Errors in long-read assemblies can critically affect protein prediction.
652 *Nat. Biotechnol.* **37** (2019), pp. 124–126.
- 653 61. G. W. Tyson, J. Chapman, P. Hugenholtz, E. E. Allen, R. J. Ram, P. M. Richardson, V. V.
654 Solovyev, E. M. Rubin, D. S. Rokhsar, J. F. Banfield, Community structure and metabolism
655 through reconstruction of microbial genomes from the environment. *Nature.* **428**, 37–43
656 (2004).
- 657 62. F. MacLeod, G. S. Kindler, H. L. Wong, R. Chen, B. P. Burns, Asgard archaea: Diversity,
658 function, and evolutionary implications in a range of microbiomes. *AIMS Microbiol.* **5**, 48–
659 61 (2019).
- 660 63. R. Zhao, J. F. Biddle, Helarchaeota and co-occurring sulfate-reducing bacteria in
661 subseafloor sediments from the Costa Rica Margin. *ISME Commun.* **1**, 25 (2021).
- 662 64. P. Offre, A. Spang, C. Schleper, Archaea in biogeochemical cycles. *Annu. Rev. Microbiol.*
663 **67**, 437–457 (2013).
- 664 65. G. Uden, J. Bongaerts, Alternative respiratory pathways of *Escherichia coli*: energetics and
665 transcriptional regulation in response to electron acceptors. *Biochim. Biophys. Acta.* **1320**,
666 217–234 (1997).
- 667 66. T. Friedrich, D. Scheide, The respiratory complex I of bacteria, archaea and eukarya and its
668 module common with membrane-bound multisubunit hydrogenases. *FEBS Lett.* **479**, 1–5
669 (2000).
- 670 67. P. S. Adam, G. E. Kolyfetis, T. L. V. Bornemann, C. E. Vorgias, A. J. Probst, Genomic
671 remnants of ancestral methanogenesis and hydrogenotrophy in Archaea drive anaerobic
672 carbon cycling. *Sci Adv.* **8**, eabm9651 (2022).
- 673 68. T. Wagner, U. Ermler, S. Shima, MtrA of the sodium ion pumping methyltransferase binds
674 cobalamin in a unique mode. *Sci. Rep.* **6**, 28226 (2016).

- 675 69. *sickle: Windowed Adaptive Trimming for fastq files using quality* (Github;
676 <https://github.com/najoshi/sickle>).
- 677 70. Y. Peng, H. C. M. Leung, S. M. Yiu, F. Y. L. Chin, IDBA-UD: a de novo assembler for
678 single-cell and metagenomic sequencing data with highly uneven depth. *Bioinformatics*. **28**,
679 1420–1428 (2012).
- 680 71. S. Nurk, D. Meleshko, A. Korobeynikov, P. A. Pevzner, metaSPAdes: a new versatile
681 metagenomic assembler. *Genome Res.* **27**, 824–834 (2017).
- 682 72. B. Langmead, S. L. Salzberg, Fast gapped-read alignment with Bowtie 2. *Nat. Methods*. **9**,
683 357–359 (2012).
- 684 73. D. D. Kang, F. Li, E. Kirton, A. Thomas, R. Egan, H. An, Z. Wang, MetaBAT 2: an
685 adaptive binning algorithm for robust and efficient genome reconstruction from
686 metagenome assemblies. *PeerJ*. **7**, e7359 (2019).
- 687 74. J. N. Nissen, J. Johansen, R. L. Allesøe, C. K. Sønderby, J. J. A. Armenteros, C. H.
688 Grønbech, L. J. Jensen, H. B. Nielsen, T. N. Petersen, O. Winther, S. Rasmussen, Improved
689 metagenome binning and assembly using deep variational autoencoders. *Nat. Biotechnol.*
690 **39**, 555–560 (2021).
- 691 75. Y.-W. Wu, B. A. Simmons, S. W. Singer, MaxBin 2.0: an automated binning algorithm to
692 recover genomes from multiple metagenomic datasets. *Bioinformatics*. **32**, 605–607 (2016).
- 693 76. D. H. Parks, M. Imelfort, C. T. Skennerton, P. Hugenholtz, G. W. Tyson, CheckM:
694 assessing the quality of microbial genomes recovered from isolates, single cells, and
695 metagenomes. *Genome Res.* **25**, 1043–1055 (2015).
- 696 77. P.-A. Chaumeil, A. J. Mussig, P. Hugenholtz, D. H. Parks, GTDB-Tk: a toolkit to classify
697 genomes with the Genome Taxonomy Database. *Bioinformatics*. **36**, 1925–1927 (2019).
- 698 78. B. Bushnell, “BBMap: A Fast, Accurate, Splice-Aware Aligner” (LBNL-7065E, Lawrence
699 Berkeley National Lab. (LBNL), Berkeley, CA (United States), 2014), (available at
700 <https://www.osti.gov/servlets/purl/1241166>).
- 701 79. X. Feng, H. Cheng, D. Portik, H. Li, Metagenome assembly of high-fidelity long reads with
702 hifiasm-meta. *Nat. Methods*. **19**, 671–674 (2022).
- 703 80. M. Kolmogorov, D. M. Bickhart, B. Behsaz, A. Gurevich, M. Rayko, S. B. Shin, K. Kuhn,
704 J. Yuan, E. Pevnikov, T. P. L. Smith, P. A. Pevzner, metaFlye: scalable long-read
705 metagenome assembly using repeat graphs. *Nat. Methods*. **17**, 1103–1110 (2020).
- 706 81. D. Hyatt, G.-L. Chen, P. F. Locascio, M. L. Land, F. W. Larimer, L. J. Hauser, Prodigal:
707 prokaryotic gene recognition and translation initiation site identification. *BMC*
708 *Bioinformatics*. **11**, 119 (2010).
- 709 82. T. Aramaki, R. Blanc-Mathieu, H. Endo, K. Ohkubo, M. Kanehisa, S. Goto, H. Ogata,

- 710 KofamKOALA: KEGG Ortholog assignment based on profile HMM and adaptive score
711 threshold. *Bioinformatics*. **36**, 2251–2252 (2020).
- 712 83. T. Paysan-Lafosse, M. Blum, S. Chuguransky, T. Grego, B. L. Pinto, G. A. Salazar, M. L.
713 Bileschi, P. Bork, A. Bridge, L. Colwell, J. Gough, D. H. Haft, I. Letunić, A. Marchler-
714 Bauer, H. Mi, D. A. Natale, C. A. Orengo, A. P. Pandurangan, C. Rivoire, C. J. A. Sigrist, I.
715 Sillitoe, N. Thanki, P. D. Thomas, S. C. E. Tosatto, C. H. Wu, A. Bateman, InterPro in
716 2022. *Nucleic Acids Res.* **51**, D418–D427 (2023).
- 717 84. D. Søndergaard, C. N. S. Pedersen, C. Greening, HydDB: A web tool for hydrogenase
718 classification and analysis. *Sci. Rep.* **6**, 34212 (2016).
- 719 85. Z. Zhou, P. Q. Tran, A. M. Breister, Y. Liu, K. Kieft, E. S. Cowley, U. Karaoz, K.
720 Anantharaman, METABOLIC: high-throughput profiling of microbial genomes for
721 functional traits, metabolism, biogeochemistry, and community-scale functional networks.
722 *Microbiome*. **10**, 33 (2022).
- 723 86. M. Shaffer, M. A. Borton, B. B. McGivern, A. A. Zayed, S. L. La Rosa, L. M. Solden, P.
724 Liu, A. B. Narrowe, J. Rodríguez-Ramos, B. Bolduc, M. C. Gazitúa, R. A. Daly, G. J.
725 Smith, D. R. Vik, P. B. Pope, M. B. Sullivan, S. Roux, K. C. Wrighton, DRAM for
726 distilling microbial metabolism to automate the curation of microbiome function. *Nucleic*
727 *Acids Res.* **48**, 8883–8900 (2020).
- 728 87. N. Dombrowski, T. A. Williams, J. Sun, B. J. Woodcroft, J.-H. Lee, B. Q. Minh, C. Rinke,
729 A. Spang, Undinarchaeota illuminate DPANN phylogeny and the impact of gene transfer on
730 archaeal evolution. *Nat. Commun.* **11**, 3939 (2020).
- 731 88. S. R. Eddy, Accelerated Profile HMM Searches. *PLoS Comput. Biol.* **7**, e1002195 (2011).
- 732 89. W. Li, K. R. O’Neill, D. H. Haft, M. DiCuccio, V. Chetvernin, A. Badretdin, G. Coulouris,
733 F. Chitsaz, M. K. Derbyshire, A. S. Durkin, N. R. Gonzales, M. Gwadz, C. J. Lanczycki, J.
734 S. Song, N. Thanki, J. Wang, R. A. Yamashita, M. Yang, C. Zheng, A. Marchler-Bauer, F.
735 Thibaud-Nissen, RefSeq: expanding the Prokaryotic Genome Annotation Pipeline reach
736 with protein family model curation. *Nucleic Acids Res.* **49**, D1020–D1028 (2021).
- 737 90. D. Santesmasses, M. Mariotti, R. Guigó, Selenoprofiles: A Computational Pipeline for
738 Annotation of Selenoproteins. *Methods Mol. Biol.* **1661**, 17–28 (2018).
- 739 91. M. Mariotti, A. V. Lobanov, R. Guigo, V. N. Gladyshev, SECISearch3 and Seblastian: new
740 tools for prediction of SECIS elements and selenoproteins. *Nucleic Acids Res.* **41**, e149
741 (2013).
- 742 92. M. Mariotti, A. V. Lobanov, B. Manta, D. Santesmasses, A. Bofill, R. Guigó, T. Gabaldón,
743 V. N. Gladyshev, Lokiarchaeota Marks the Transition between the Archaeal and Eukaryotic
744 Selenocysteine Encoding Systems. *Mol. Biol. Evol.* **33**, 2441–2453 (2016).
- 745 93. P. P. Chan, B. Y. Lin, A. J. Mak, T. M. Lowe, tRNAscan-SE 2.0: improved detection and
746 functional classification of transfer RNA genes. *Nucleic Acids Res.* **49**, 9077–9096 (2021).

- 747 94. B. A. Sweeney, D. Hoksza, E. P. Nawrocki, C. E. Ribas, F. Madeira, J. J. Cannone, R.
748 Gutell, A. Maddala, C. D. Meade, L. D. Williams, A. S. Petrov, P. P. Chan, T. M. Lowe, R.
749 D. Finn, A. I. Petrov, R2DT is a framework for predicting and visualising RNA secondary
750 structure using templates. *Nat. Commun.* **12**, 1–12 (2021).
- 751 95. D. Santesmasses, M. Mariotti, R. Guigó, Computational identification of the selenocysteine
752 tRNA (tRNA^{Sec}) in genomes. *PLoS Comput. Biol.* **13**, e1005383 (2017).
- 753 96. M. R. Olm, C. T. Brown, B. Brooks, J. F. Banfield, dRep: a tool for fast and accurate
754 genomic comparisons that enables improved genome recovery from metagenomes through
755 de-replication. *ISME J.* **11**, 2864–2868 (2017).
- 756 97. A. Crits-Christoph, *filter_reads.py: Filters BAM files created by bowtie2 for better read*
757 *mapping. Use for genomes from metagenomes* (Github;
758 https://github.com/alexcritschristoph/filter_reads.py).
- 759 98. R. McClure, D. Balasubramanian, Y. Sun, M. Bobrovskyy, P. Sumby, C. A. Genco, C. K.
760 Vanderpool, B. Tjaden, Computational analysis of bacterial RNA-Seq data. *Nucleic Acids*
761 *Res.* **41**, e140 (2013).
- 762 99. B. J. Baker, J. H. Saw, A. E. Lind, C. S. Lazar, K.-U. Hinrichs, A. P. Teske, T. J. G. Ettema,
763 Genomic inference of the metabolism of cosmopolitan subsurface Archaea, Hadesarchaea.
764 *Nat Microbiol.* **1**, 16002 (2016).
- 765 100. A. E. Darling, G. Jospin, E. Lowe, F. A. Matsen 4th, H. M. Bik, J. A. Eisen, PhyloSift:
766 phylogenetic analysis of genomes and metagenomes. *PeerJ.* **2**, e243 (2014).
- 767 101. M. Mirdita, K. Schütze, Y. Moriwaki, L. Heo, S. Ovchinnikov, M. Steinegger,
768 ColabFold: making protein folding accessible to all. *Nat. Methods.* **19**, 679–682 (2022).
- 769 102. E. C. Meng, T. D. Goddard, E. F. Pettersen, G. S. Couch, Z. J. Pearson, J. H. Morris, T.
770 E. Ferrin, UCSF ChimeraX: Tools for structure building and analysis. *Protein Sci.* **32**,
771 e4792 (2023).
- 772 103. H. M. Berman, J. Westbrook, Z. Feng, G. Gilliland, T. N. Bhat, H. Weissig, I. N.
773 Shindyalov, P. E. Bourne, The Protein Data Bank. *Nucleic Acids Res.* **28**, 235–242 (2000).
- 774 104. C. J. Chastain, C. J. Failing, L. Manandhar, M. A. Zimmerman, M. M. Lakner, T. H. T.
775 Nguyen, Functional evolution of C(4) pyruvate, orthophosphate dikinase. *J. Exp. Bot.* **62**,
776 3083–3091 (2011).
- 777 105. W. Buckel, H. A. Barker, Two pathways of glutamate fermentation by anaerobic bacteria.
778 *J. Bacteriol.* **117**, 1248–1260 (1974).
- 779 106. T. J. Williams, M. Allen, B. Tschitschko, R. Cavicchioli, Glycerol metabolism of
780 haloarchaea. *Environ. Microbiol.* **19**, 864–877 (2017).
- 781 107. K. Okamura-Ikeda, Y. Ohmura, K. Fujiwara, Y. Motokawa, Cloning and nucleotide

- 782 sequence of the gcv operon encoding the Escherichia coli glycine-cleavage system. *Eur. J.*
783 *Biochem.* **216**, 539–548 (1993).
- 784 108. T. J. Lie, K. C. Costa, B. Lupa, S. Korpole, W. B. Whitman, J. A. Leigh, Essential
785 anaplerotic role for the energy-converting hydrogenase Eha in hydrogenotrophic
786 methanogenesis. *Proc. Natl. Acad. Sci. U. S. A.* **109**, 15473–15478 (2012).
- 787 109. P. Pedroni, A. Della Volpe, G. Galli, G. M. Mura, C. Pratesi, G. Grandi, Characterization
788 of the locus encoding the [Ni-Fe] sulfhydrogenase from the archaeon *Pyrococcus furiosus*:
789 evidence for a relationship to bacterial sulfite reductases. *Microbiology.* **141 (Pt 2)**, 449–
790 458 (1995).
- 791 110. C. Greening, A. Biswas, C. R. Carere, C. J. Jackson, M. C. Taylor, M. B. Stott, G. M.
792 Cook, S. E. Morales, Genomic and metagenomic surveys of hydrogenase distribution
793 indicate H₂ is a widely utilised energy source for microbial growth and survival. *ISME J.*
794 **10**, 761–777 (2016).
- 795 111. T. Wagner, J. Koch, U. Ermler, S. Shima, Methanogenic heterodisulfide reductase
796 (HdrABC-MvhAGD) uses two noncubane [4Fe-4S] clusters for reduction. *Science.* **357**,
797 699–703 (2017).
- 798 112. V. Müller, New Horizons in Acetogenic Conversion of One-Carbon Substrates and
799 Biological Hydrogen Storage. *Trends Biotechnol.* **37**, 1344–1354 (2019).
- 800 113. S. T. Cole, K. Eiglmeier, S. Ahmed, N. Honore, L. Elmes, W. F. Anderson, J. H. Weiner,
801 Nucleotide sequence and gene-polypeptide relationships of the glpABC operon encoding
802 the anaerobic sn-glycerol-3-phosphate dehydrogenase of Escherichia coli K-12. *J.*
803 *Bacteriol.* **170**, 2448–2456 (1988).
- 804 114. D. P. Bojanova, V. Y. De Anda, M. A. Haghnegahdar, A. P. Teske, J. L. Ash, E. D.
805 Young, B. J. Baker, D. E. LaRowe, J. P. Amend, Well-hidden methanogenesis in deep,
806 organic-rich sediments of Guaymas Basin. *ISME J.* **17**, 1828–1838 (2023).

807
808
809
810
811
812
813
814
815
816
817
818
819
820

821 **Acknowledgments:** We thank Basem Al-Shayeb for his contribution to field work and generation
822 of sequence datasets, and Shufei Lei and Jordan Hoff for bioinformatics support. We thank Dr.
823 Chris Greening and Dr. Pok Leung for discussions on archaeal hydrogenases classification. We
824 also thank Adam Panagiotis for the helpful discussion about methyltransferases from
825 methanogens. Lastly, we are grateful to Dr. Luke Oltrogge and Dr. Daniel Gittins for their
826 discussions about the multimeric structures modeled using AlphaFold.

827
828 **Funding:** This publication is based on research in part funded by the Bill & Melinda Gates
829 Foundation (Grant Number: INV-037174 to JFB). The findings and conclusions contained within
830 are those of the authors and do not necessarily reflect positions or policies of the Bill & Melinda
831 Gates Foundation University of California Dissertation-Year Fellowship (to LEVA). Stengl-Wyer
832 Graduate Fellowship and University of Texas at Austin Graduate Continuing Fellowship (to KEA).
833 Innovative Genomics Institute. Moore-Simons Project on the Origin of the Eukaryotic Cell,
834 Simons Foundation grant 73592LPI (<https://doi.org/10.46714/735925LPI>) (BJB) and Simons
835 Foundation early career award 687165 (BJB).

836

837 **Author contributions:**

838 Brackets denote equal contribution in the author list order. The study was designed by LEVA and
839 JFB. Samples collection and nucleic acid extractions were performed by L.E.V.A., M.C.S, J.F.B.,
840 A.C.C., J.W.R. and L.D.S., Metagenomic data was generated by L.E.V.A., M.C.S., R.S., A.C.C.,
841 J.W.R., and J.F.B. Genome binning was done by J.F.B., L.E.V.A., M.C.S., A.C.C, and J.W.R.
842 Complete Asgard genome curation was conducted by J.F.B. and L.E.V.A. Phylogenetic analyses
843 were conducted by (KEA and LEVA). Metabolic annotation and analysis done by (LEVA, KEA,
844 and V.D.A.), M.C.S provided knowledge on metabolism of archaea. V.K. performed tRNAs and
845 selenoproteins analysis. D.S. and B.J.B. provided feedback on the study design and methodology.
846 J.F.B., D.S, and B.J.B. provided resources and funding. L.E.V.A. and J.F.B. wrote the manuscript,
847 with significant contributions by K.E.A., V.D.A, M.C.S and input from all authors. All authors
848 read and approved the manuscript.

849

850 **Competing interests:** JFB is a co-founder of Metagenomi. The other authors declare that they
851 have no competing interests.

852

853 **Data and materials availability:** Prior to publication, the genomes reported in this study can be
854 accessed via https://ggkbase.berkeley.edu/SRVP_asgard/organisms.

855

856

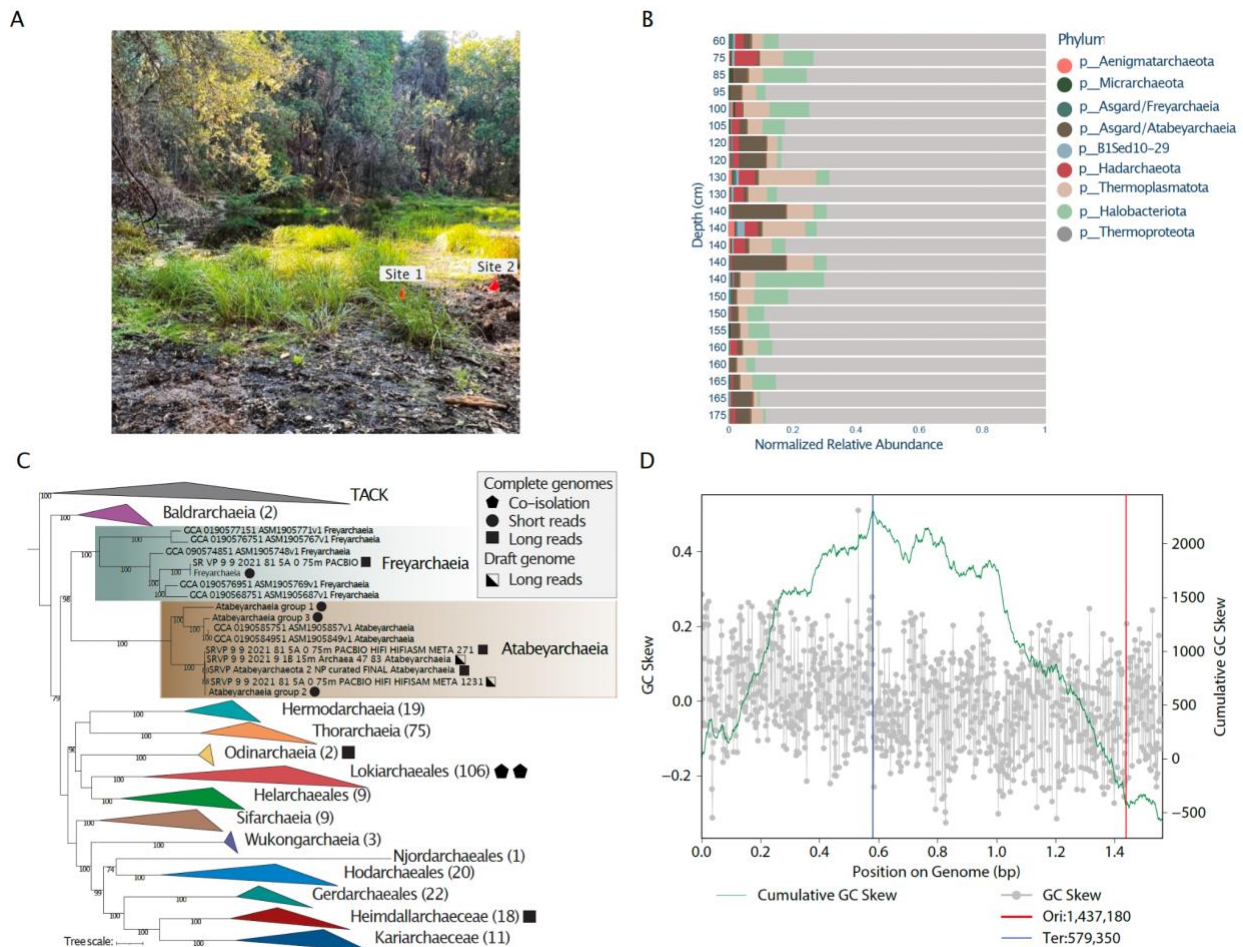
857

858

859

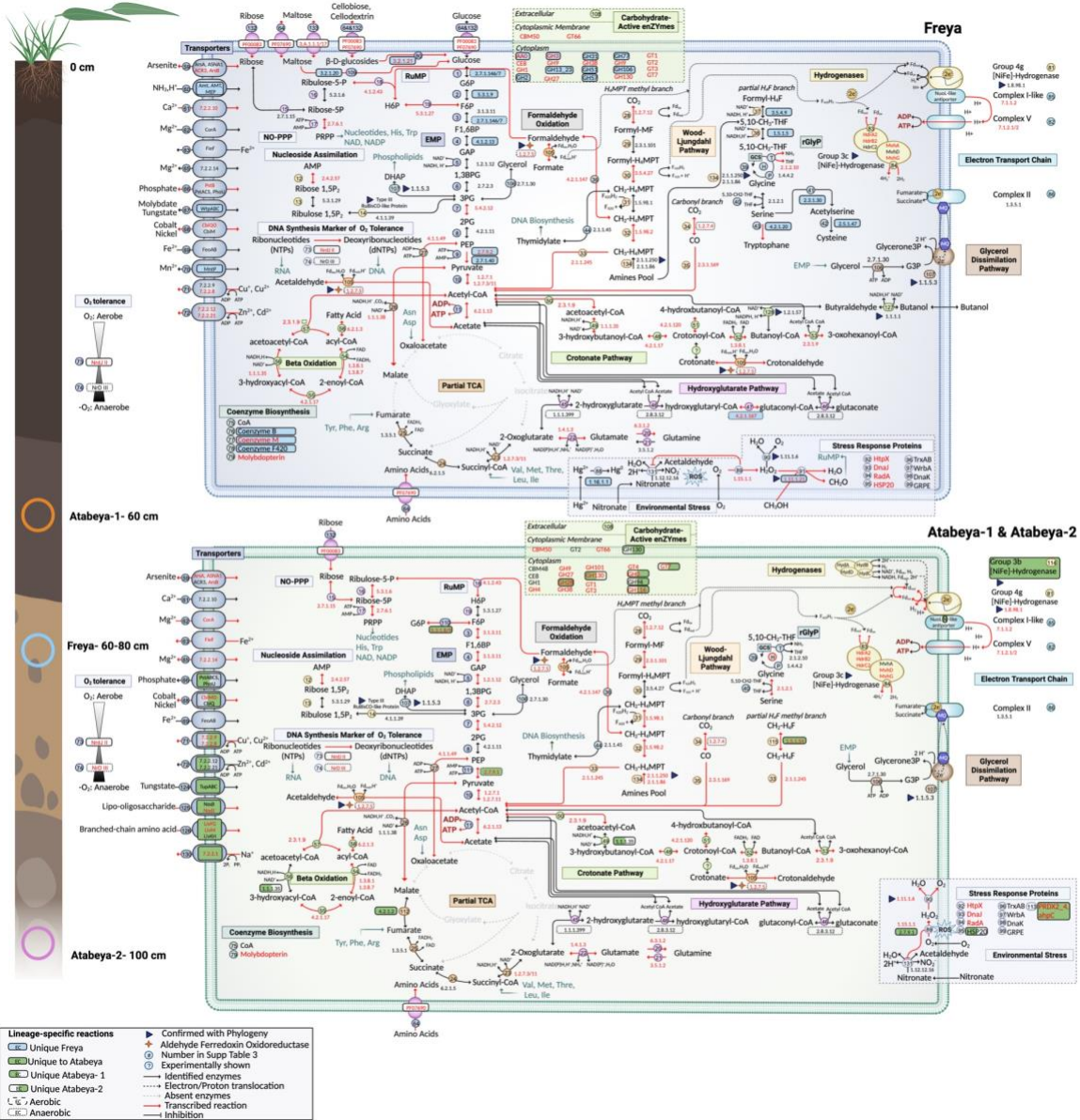
860

861 **Figure 1 Archaea dominate deep regions of wetland soil and host novel Asgard archaea A.**
 862 Photograph of the vernal pool that was metagenomically sampled in this study, in Lake County,
 863 California, USA. **B.** Archaeal genomic abundance excluding bacterial genomes. **C.** Phylogenetic
 864 distribution of Asgard Archaea complete genomes. The maximum-likelihood phylogeny was
 865 generated with Iqtree v1.6.1, utilizing 47 concatenated archaeal Clusters of Orthologous Groups
 866 of proteins (arCOGs). The best-fit model was determined as LG+F+R10 based on the Bayesian
 867 Information Criterion. Non-parametric bootstrapping was conducted with 1,000 replicates for
 868 robustness. The filled-in square, circle, and triangle indicate closed complete genomes from short
 869 reads, published complete genomes from long reads, and genomes from co-isolated cultured
 870 representatives, respectively. The pentagon highlights the long read draft genomes from this site
 871 (PacBio or Nanopore). **D.** Bidirectional replication indication in Atabayarchaeia complete
 872 genomes. The GC skew is shown as a grey plot overlaying the cumulative GC skew, presented as
 873 a green line. The blue lines mark the predicted replication terminus.



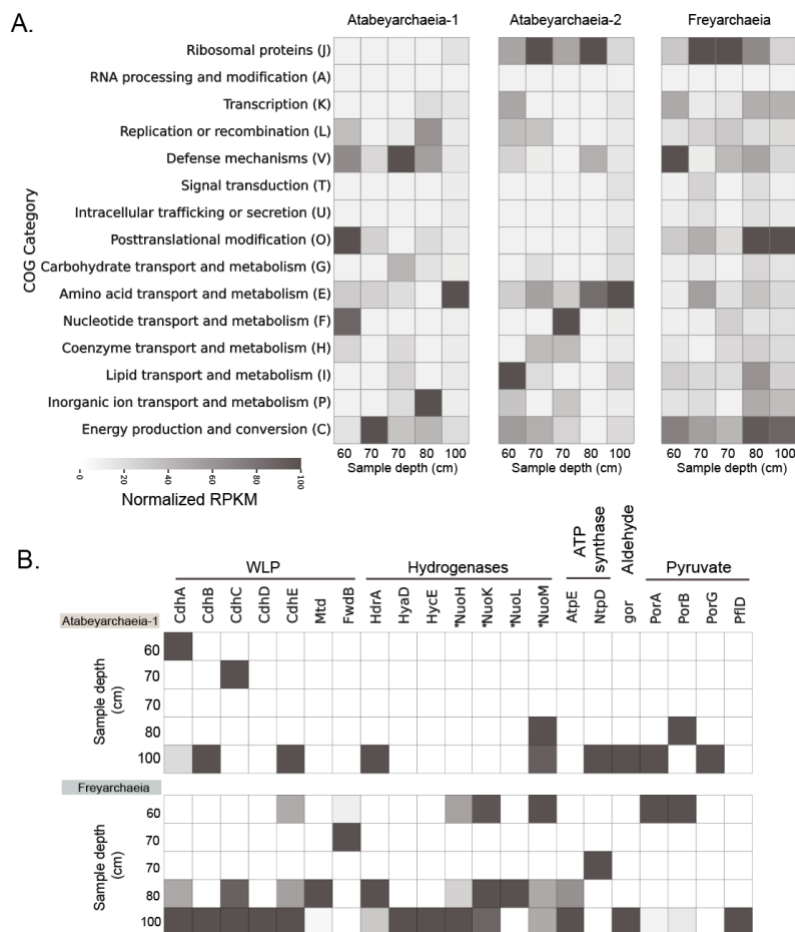
876

877 **Figure 2 Metabolic capacities of terrestrial Atabayarchaeia and Freyarchaeia for overall**
 878 **implications for biogeochemical cycling in wetlands.** Inference of the pathways from the
 879 complete genomes is based on the comparison of predicted proteins with a variety of functional
 880 databases (“see materials and methods”). The extraction depth location within the cores is shown
 881 on the left. All reactions are numbers and correspond to **table S7**. EC/TCDB numbers shaded fully
 882 or partially in blue or green are unique to the lineages and complete genomes, whereas the dashed
 883 boxes distinguish oxygen-sensitive enzymes. The multi-functional aldehyde ferredoxin
 884 oxidoreductase is shown with a star. Proteins marked with a triangle have generated phylogenies
 885 to determine their evolutionary histories and substrate specificity. Reactions with mapped
 886 transcripts are denoted with red text and arrows. Created using BioRender.com.
 887



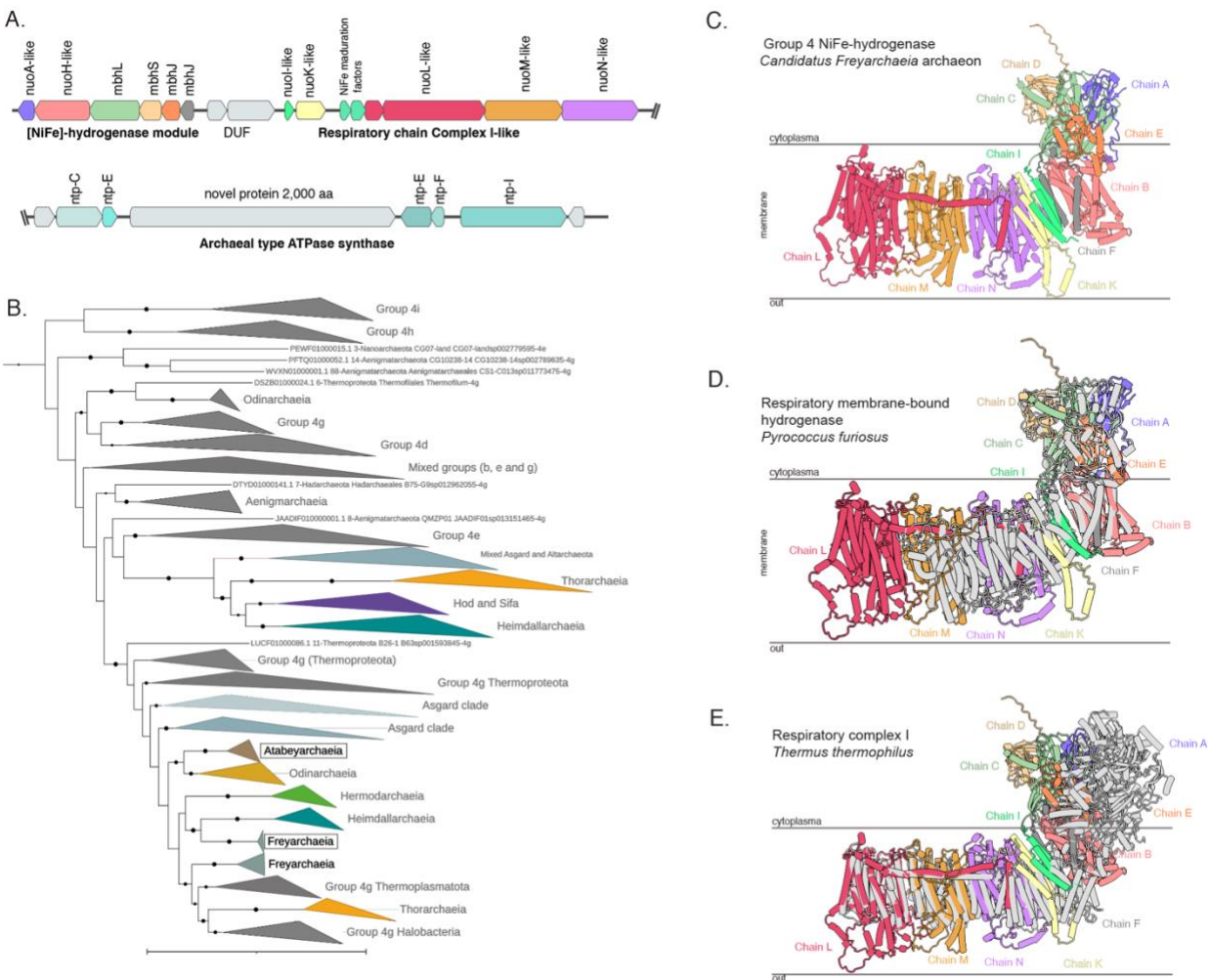
888
889

890 **Figure 3. Metatranscriptomic profiling of soil-associated Asgard archaeal genomes A.**
 891 Heatmap visualization of normalized Reads Per Kilobase per Million mapped reads (RPKM)
 892 values for ORFs with high sequence similarity ($\geq 95\%$) to the genomes of Atabeyarchaeia-1,
 893 Atabeyarchaeia-2, and Freyarchaeia, across various soil depths. A total of 2,191 open reading
 894 frames (ORFs) were categorized using the Clusters of Orthologous Groups (COG) database, with
 895 Atabeya-1, Atabeya-2, and Freya expressing 465, 804, and 922 unique ORFs, respectively. The
 896 ORFs were annotated and assigned to 15 COG categories, indicating the functional potential of
 897 each archaeal genome in situ. Columns represent metatranscriptomes from different soil depths,
 898 highlighting the spatial variability in the expression of key metabolic and cellular processes. **B.**
 899 Expanded heatmap of Atabeyarchaeia-1 and Freyarchaeia expressed genes under the category C:
 900 Energy production and conversion. Key genes of the WLP (CODH/ACS, carbon monoxide
 901 dehydrogenase/acetyl-CoA synthase; *fwdB*, formate dehydrogenase; *mtd*, 5,10-methylene-H4-
 902 methanopterin dehydrogenase), hydrogenases and associated genes (*HdrA*, heterodisulfide
 903 reductase and group NiFe-hydrogenase; *Mvh*, methyl viologen reducing hydrogenase); *HyaD*
 904 (NiFe-hydrogenase_maturating_factor); *HycE* and *Nuo* like subunits, (group 4 NiFe-
 905 hydrogenase), ATP synthase (*AtpE*, V/A-type H⁺/Na⁺-transporting ATPase subunit_K; *NtpD*,
 906 V/A-type H⁺/Na⁺ transporting ATPase subunit D) and aldehyde metabolism (*gor*,
 907 Aldehyde:ferredoxin oxidoreductases), pyruvate oxidation (*porABCD*, 2-pyruvate:ferredoxin
 908 oxidoreductase; *pflD*, pyruvate-formate lyase).
 909
 910



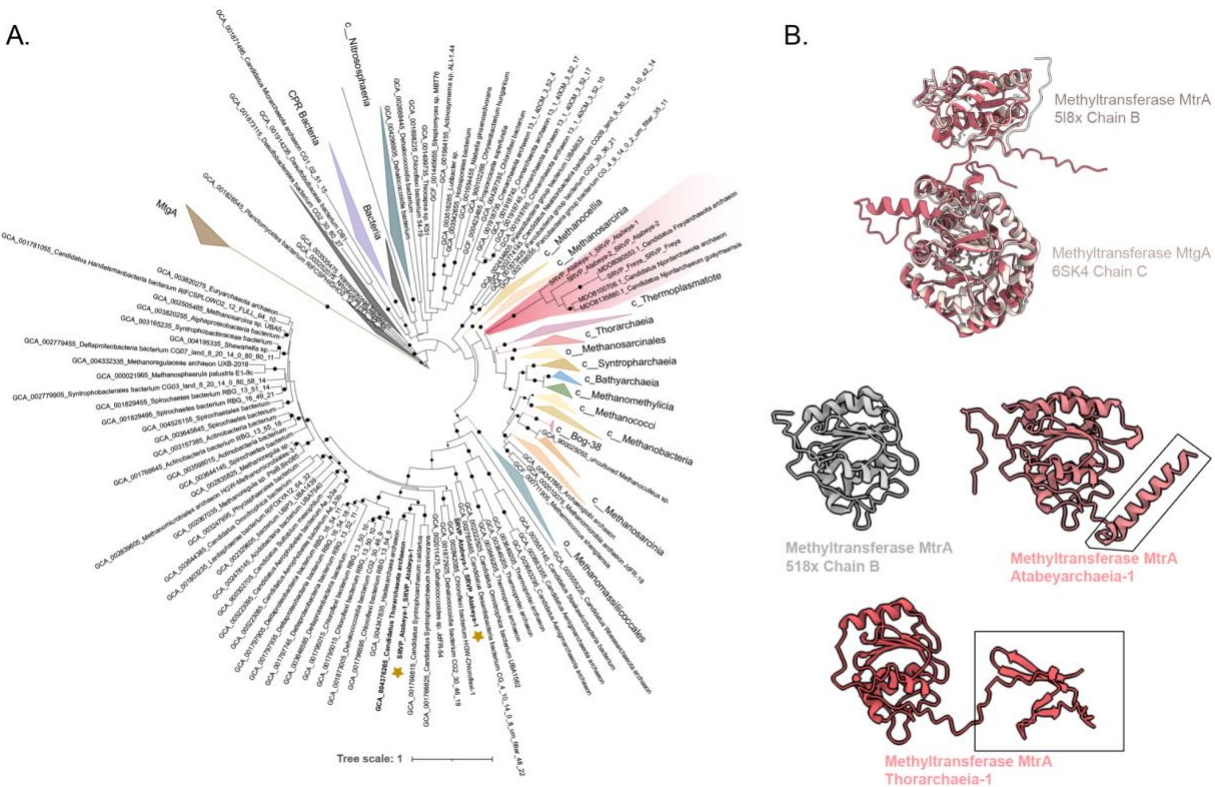
911

912 **Figure 4. Phylogeny, genetic organization and structure of the novel group 4 energy-**
 913 **conservation complex I-like NiFe-hydrogenase from Asgard archaea A.** Genetic organization
 914 of the group 4 [NiFe]-hydrogenase module, the proton-translocating membrane module, and ATP
 915 synthase from the Freyarchaeia genome. **B.** Maximum likelihood phylogeny of group 4 [NiFe]-
 916 hydrogenase large subunit from Asgard archaea and reference sequences. The bolded taxonomic
 917 groups highlight the clades with genomes from this study used for modeling. **C.** AlphaFold models
 918 of [NiFe]-hydrogenase module and the proton-translocating membrane module where each
 919 candidate subunit is represented by a different color based on the best subunit matched. **D.**
 920 AlphaFold model of Freyarchaeia hydrogenase complex colored by chains, aligned with cryoEM
 921 structure of a respiratory membrane-bound hydrogenase (MBH) from *Pyrococcus furiosus* (27)
 922 (PDB ID: 5L8X). **E.** AlphaFold model of Freyarchaeia hydrogenase complex colored by chains,
 923 aligned with Crystal structure of respiratory complex I from *Thermus thermophilus*(31) (PDB:
 924 4HEA).
 925
 926



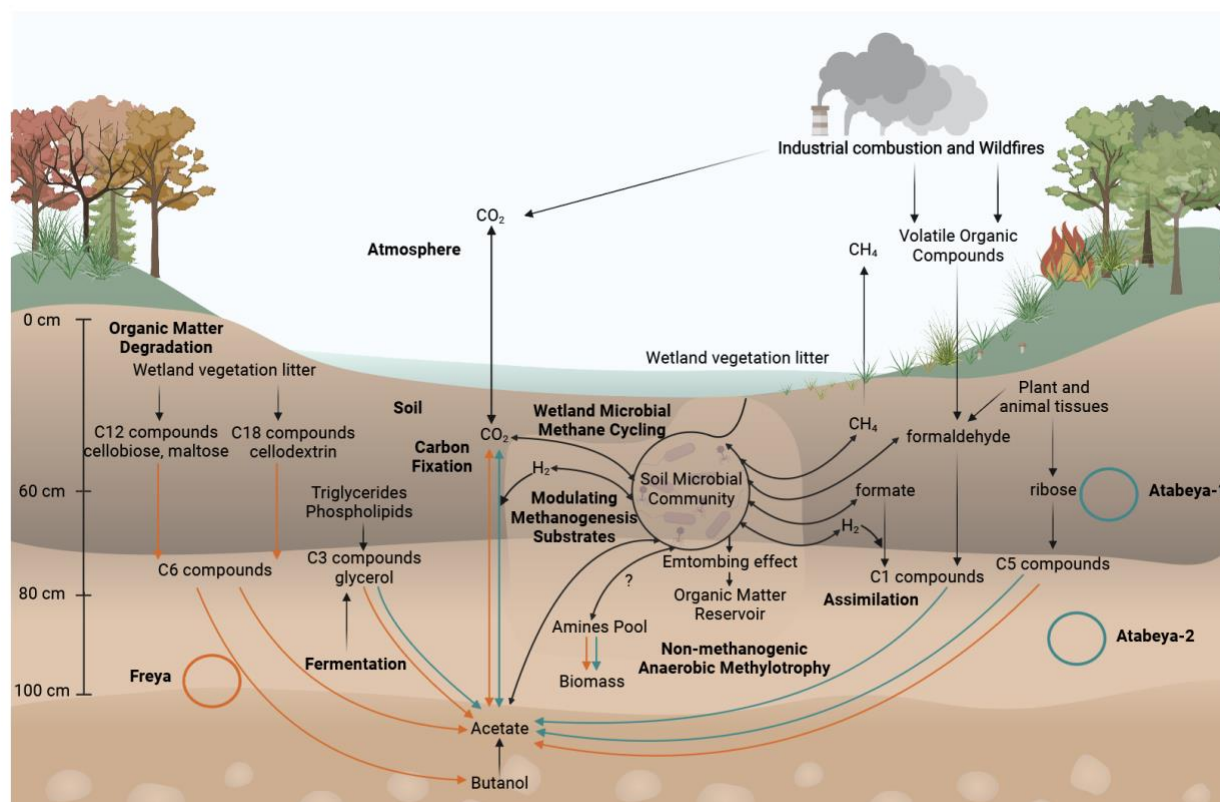
927
 928
 929
 930

931 **Figure 5** Non-methanogenic MtrA, MtrH and MtrAH fusion methyltransferases **A.** Maximum
 932 likelihood phylogeny of MtrA and the MtrAH fusion, with reference to Tetrahydromethanopterin
 933 S-methyltransferase subunit A (MtrA) with the closest corresponding domains being MtrA from
 934 the characterized Tetrahydromethanopterin S-methyltransferase subunit A (MtrA) protein (PDB
 935 ID: 5L8X) (67). The coral colored clade is the novel fusion present in Atabayarchaeia, Freyarchaeia
 936 and other Asgardarchaeota members. **B.** AlphaFold models of Atabayarchaeia-1 MtrAH (fusion)
 937 in coral aligned with the grey corresponding domains of the characterized protein
 938 Tetrahydromethanopterin S-methyltransferase subunit A (MtrA) (PDB ID: 5L8X)(68) and
 939 Methyltransferase (MtgA) from *Desulfitobacterium hafniense* in complex with methyl-
 940 tetrahydrofolate (PDB ID: 6SK4) at the N terminus. We also modeled the putative MtrA present
 941 in Atabayarchaeia-1 with the closest corresponding domains being MtrA from the characterized
 942 Tetrahydromethanopterin S-methyltransferase subunit A (MtrA) protein (PDB ID: 5L8X).
 943



944
 945
 946
 947
 948
 949
 950
 951
 952
 953
 954
 955

956 **Figure 6. Overview of the wetland soil dynamics and biogeochemical cycling in**
957 **Atabeyarchaeia and Freyarchaeia.** Complete genomes for Atabeyarchaeia and Freyarchaeia are
958 shown with green and orange circles, respectively. 2 Atabeyarchaeia genomes (Atabeya-1 and
959 Atabeya-2) and 1 Freyarchaeia (Freya) genome were isolated and carefully curated and closed
960 from wetland soil between 60-100 cm. These anaerobic lineages were shown in this study to
961 encode the Wood-Ljungdahl Pathway for CO₂ fixation (e.g. methylated compounds such as
962 quaternary amines) and EMP Pathway, components of chemolithotrophy and heterotrophy,
963 producing acetate shown in arrows (green and orange), corresponding to the genome colors.
964 Additionally, these lineages are involved in modulating methanogenesis substrates in these
965 wetland soils. Detailed description of the specific pathways is found in main text, **Fig. 2**, and
966 supplementary materials. Created using BioRender.com.
967



968
969
970
971
972
973
974
975
976
977
978
979
980